Supporting Information

Proteomic profiling of antimalarial plasmodione using 3-benz(o)ylmenadione affinity-based probes

Ilaria Iacobucci,[a],[b],[c],# Vittoria Monaco,[a],[b],[c],# Agnès Hovasse,[b] Baptiste Dupouy,[a] Rodrigue Keumoe,[d] Bogdan Cichocki,[a] Mourad Elhabiri,[a] Brigitte Meunier,[e] Jean-Marc Strub,[b] Maria Monti,[c] Sarah Cianférani,[b] Stéphanie A. Blandin,[d] Christine Schaeffer-Reiss,[b] Elisabeth Davioud-Charvet[a],*

# authors contributed equally as first co-authors

[a] Ilaria Iacobucci, Vittoria Monaco, Baptiste Dupouy, Bogdan Cichocki, Mourad Elhabiri, Elisabeth Davioud-Charvet − UMR7042 CNRS-Université de Strasbourg-Université Haute-Alsace, Laboratoire d'Innovation Moléculaire et Applications (LIMA), Team Bio(IN)organic & Medicinal Chemistry, European School of Chemistry, Polymers and Materials (ECPM), 25, rue Becquerel, F-67087 Strasbourg, France; orcid.org/0000-0001-7026-4034;

[b] Agnès Hovasse, Jean-Marc Strub, Sarah Cianférani, Christine Schaeffer-Reiss, 1) Laboratoire de Spectrométrie de Masse Bio Organique, IPHC UMR 7178 CNRS-Université de Strasbourg, 67087 Strasbourg, France; 2) Infrastructure Nationale de Protéomique ProFI - FR2048, 67087 Strasbourg, France

[c] Maria Monti, University of Naples "Federico II", Department of Chemical Sciences, Complesso Universitario di Monte Sant' Angelo, Via Cintia 26, I-80126 Napoli

[d] Rodrigue Keumoe, Stéphanie A. Blandin, INSERM U1257 - CNRS UPR9022 - Université de Strasbourg, Institut de Biologie Moléculaire et Cellulaire, Strasbourg, France

[e] Brigitte Meunier, Institute for Integrative Biology of the Cell (I2BC), CEA, CNRS, Univ. Paris-Sud, Université Paris-Saclay, 91198 Gif-sur-Yvette cedex, France.

Table of contents:

Appendix: Reporting Experimental Information and Data

A. Synthetic Procedures

Optimized synthesis of photoreactive 'clickable' 3-benz(o)ylmenadiones 1 and 4

The synthetic route to prepare the benzoylMD probe **1**, originally described in ref.[19] (under the compound code **7**) was optimized. Here, instead of performing the Friedel-Crafts acylation of the starting 2-methyl-1,4-dimethoxynaphthalene using 4-iodobenzoic acid, which leads to the formation of other regioisomers,[25] the first step was performed using 4-bromobenzoic acid, generating fewer regioisomers. This improved modification is compatible with the next step, leading to **9** with a 76% overall yield instead of a 31% overall yield with the initial protocol (Scheme S1).

To synthetize the benzoylMD derivatives **1** (R_1 = H) and **3** (R_1 = F), menadione or 6-F-menadione were first reduced and protected using dimethylsulfate yielding **7** (R_1 = H) or **11** (R_1 = F). Then, Friedel-Crafts acylations using 4-bromobenzoic acid were performed forming **8** (R_1 = H) or **12** (R_1 = F). The following steps were kept unchanged from the benzyl synthetic route: Sonogashira reaction yielding **9** (R_1 = H) or **13** (R_1 = F), TMS deprotection producing **10** (R_1 = H) or **14** (R_1 = F) and oxidative demethylation forming final benzoylMD probes **1** (R_1 = H) or **3** (R_1 = F) with 76% or 40% overall yields (4 steps), respectively (Scheme S1).

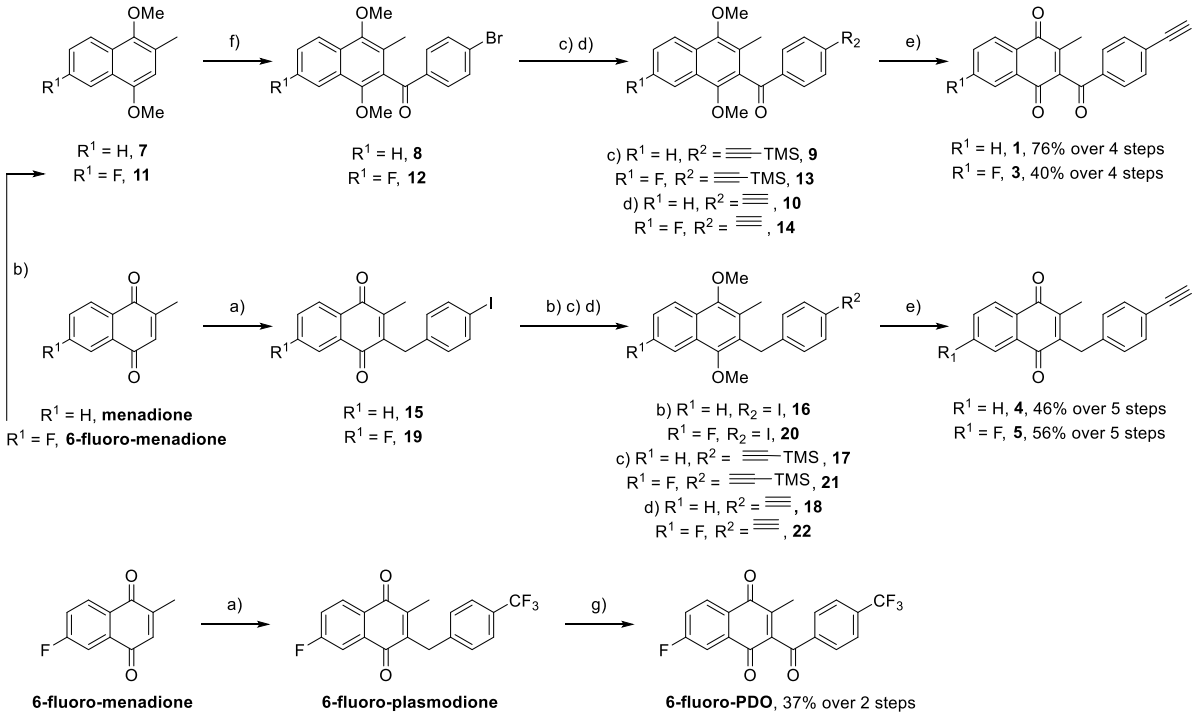

Scheme S1 Synthesis of clickable 6-H and 6-fluoro-3-benzylMD with 6-H and 6-fluoro-3-benzoylMDalkyne probes and of the 6-fluoro-PDO. a) 4-iodophenylacetic acid or 4-(trifluoromethyl)acetic acid, $AgNO_3$, $(NH_4)_2S_2O_8$, CH_3CN:H_2O, reflux, 4 h; b) 1. $SnCl_2$, HCl, EtOH, rt, 2 h, 2. Me_2SO_4, acetone, KOH, MeOH, 60 °C, 4 h; c) ethynyltrimethylsilane, CuI, $Pd(PPh_3)_2Cl_2$, NEt_3, 70 °C, 20 h; d) TBAF, THF, rt, 1.5 h; e) CAN, CH_3CN:H_2O, rt, 1 h. f) 4-bromobenzoic acid, TFAA, TfOH, DCM, 16 h; g) DCM, propan-2-ol, O_2, UV, 72 h.

The clickable benzylMD probe **4** was synthesized using the reported synthetic route previously described[19] (Scheme 1). To obtain both benzylMDs alkyne derivatives **4** (R_1 = H) and **5** (R_1 = F), menadione or 6-F-menadione were first engaged to a Kochi-Anderson reaction with 4-iodophenylacetic

acid producing **15** (R_1 = H) or **19** (R_1 = F). BenzylMDs were reduced with $SnCl_2$ in acid medium, and then protected by methylation using dimethylsulfate leading to **16** (R_1 = H) or **20** (R_1 = F). Iodo intermediates were submitted to a Sonogashira pallado-cross coupling reaction, forming **17** (R_1 = H) or **21** (R_1 = F). TMS groups were removed by TBAF producing free terminal alkynes **18** (R_1 = H) or **22** (R_1 = F). Finally, 1,4-quinone moieties were recovered by oxidative demethylation following addition of CAN to obtain **4** (R_1 = H) or **5** (R_1 = F) with 46% or 56% overall yields (5 steps), respectively.

B. Characterization

B1. Characterization of Compounds & Materials

Chemistry. General. All the reagents and solvents were purchased from commercial sources and used as received, unless otherwise stated. The ^1H, ^{19}F and ^{13}C {^1H} NMR spectra were obtained in $CDCl_3$ as solvents using a 400 MHz or a 500 MHz spectrometer. Chemical shifts were reported in parts per million (δ). ^1H NMR data were reported as follows: chemical shift (δ ppm) (multiplicity, coupling constant (Hz), and integration). Multiplicities are reported as follows: s = singlet, d = doublet, t = triplet, q = quartet, m = multiplet, or combinations thereof. High-resolution mass spectroscopy (HRMS) spectra were recorded using the electron spray ionization (ESI) technique.

Synthesis of precursors. Reactants and building blocks were purchased from commercial sources, such as Fluorochem, Sigma-Aldrich and Alfa Aesar. 1,4-dimethoxy-2-methyl-naphthalene **7** was synthesized according to the previously published method. [37]

B1.1. Synthesis of known probes 1 and 4 with improved procedures:

Synthesis of Probe 1 in bulk (Cpd 7 in [19])

(4-bromophenyl)(1,4-dimethoxy-3-methylnaphthalen-2-yl)methanone 8. Synthesized according to the previously published method (for Cpd 2k in [25]) from 1,4-dimethoxy-2-methylnaphthalene (1 g, 4.9 mmol, 1 equiv.) and 4-bromobenzoic acid (1.5 g, 7.4 mmol, 1.5 equiv.). The reaction crude was not purified and was directly engaged in the next reaction. (1,4-dimethoxy-3-methylnaphthalen-2-yl)(4-((trimethylsilyl) ethynyl)phenyl)methanone 9. Compound 8 (1.4 g, 3.7 mmol, 1 equiv.) was dissolved under argon in triethylamine (85 mL) in a dry double necked round bottom flask at room temperature. Then, $Pd(PPh_3)_2(Cl)_2$ (130 mg, 0.2 mmol, 0.05 equiv.), CuI (70 mg, 0.3 mmol, 0.1 equiv.) were added under argon and three cycles argon vacuum were performed, finally trimethylsilylacetylene (1.6 mL, 11.1 mmol, 3 equiv.) was added. The round bottom flask was stirred at 70 °C for 24 h. The reaction mixture was quenched with a 1/1 brine/water mixture and the aqueous phase was extracted three times with ethyl acetate, dried over magnesium sulfate and solvent was removed under vacuum. The crude was purified by silica gel chromatography (CHX/T, 2/8, v/v, UV) to afford the desired product 9 as a yellow oil (1.3 g, 87.3%). The product analysis was in accordance with that of Cpd 7c in [19]. (1,4-dimethoxy-3-methylnaphthalen-2-yl)(4-ethynylphenyl)methanone 10. Synthesized from compound 9 according to the previously published method. The product analysis was in accordance with that of Cpd 7d in [19]). 2-(4-ethynylbenzoyl)-3-methylnaphthalene-1,4-dione 1. The desired product was synthesized from compound 10 according to the previously published method, purified with eluent (CHX/EtOAc, 9/1, v/v, UV, Rf = 0.4), and isolated as a yellow solid, 88%. The product analysis was in accordance with that of Cpd 7 in [19]). ^1H NMR (400 MHz, $CDCl_3$) δ 8.23 – 8.13 (m, 1H), 8.09 – 8.04 (m, 1H), 7.90 – 7.83 (m, 2H), 7.83 – 7.75 (m, 2H), 7.65 – 7.54 (m, 2H), 3.29 (s, 1H), 2.06 (s, 3H).

Synthesis of Probe 4 in bulk (Cpd 11 in [19]):

2-(4-iodobenzyl)-3-methylnaphthalene-1,4-dione 15 (Cpd **11a** in [19])**.** Synthesized from menadione according to the previously published method, but without any purification, the crude mixture was directly engaged in the next step. **2-(4-iodobenzyl)-1,4-dimethoxy-3-methylnaphthalene 16.** Synthesized from **15** according to the previously published method (Cpd **11b** in [19]), but without any purification, the crude mixture was directly engaged in the next step. **((4-((1,4-dimethoxy-3-methylnaphthalen-2-yl)methyl)phenyl)ethynyl)trimethyl-silane 17** (Cpd **11c** in [19])**.** Synthesized from **16** according to the previously published method) but without any purification, the crude mixture was directly engaged in the next step. **2-(4-ethynylbenzyl)-1,4-dimethoxy-3-methylnaphthale-ne 18** (Cpd **11d** in [19])**.** Synthesized from **17** according to the previously published method, but without any purification, the crude mixture was directly engaged in the next step. **2-(4-ethynylbenzyl)-3-methylnaphthalene-1,4-dione 4** (Cpd **11** in [19])**.** The desired product was synthesized from compound **18** according to the previously published method, purified with eluant (CHX/EtOAc, 8/2, v/v, UV, Rf = 0.3), and isolated as a yellow solid, 46% overall yield (over 5 steps). ^{1}H NMR (400 MHz, $CDCl_3$) δ 8.18 – 8.03 (m, 2H), 7.71 (dd, *J* = 5.8, 3.3 Hz, 2H), 7.44 – 7.30 (m, 2H), 7.22 – 7.14 (m, 2H), 4.03 (s, 2H), 3.03 (s, 1H), 2.23 (s, 3H).

B1.2. Synthesis of new probes 3 and 5:

Synthesis of probe 3

6-fluoro-1,4-dimethoxy-2-methylnaphthalene 11. 6-fluoro-menadione (1.5 g, 7.9 mmol, 1 equiv.), was solubilized in MeOH (30 mL) then a solution of tin chloride (3.7 g, 19.7 mmol, 2.5 equiv.) in 37% aqueous HCl (2.7 mL, 32.5 mmol, 4.1 equiv.) was added dropwise and the mixture was stirred 30 min at room temperature until the solution came back yellowish. Most of the solvent were evaporated under vacuum, the yellow precipitate was rinsed with water. The powder was dissolved in acetone (30 mL) and dried over magnesium sulfate. Under argon, dimethyl sulfate (3.7 mL, 39.4 mmol, 5 equiv.) was added to the previous mixture then a solution of KOH (2.2 g, 39.4 mmol, 5 equiv.) in MeOH (7.5 mL) was added drop by drop. When the addition was completed the mixture was stirred at reflux 60 °C during 1 h. A 20% aqueous solution of KOH (20 mL) was added to the mixture and organic solvent were removed under vacuum. The aqueous phase was extracted three times with dichloromethane, dried over magnesium sulfate and solvent was removed under vacuum (CHX/T, 5/5, v/v, UV, Rf = 0.6). The crude residue gives the desired product **11** (1.5 g, 86.3%) as a beige solid, M.p. = 52-53 °C. ^{1}H NMR (400 MHz, $CDCl_3$) δ 8.07 (dd, *J* = 9.2, 5.6 Hz, 1H), 7.88 (dd, *J* = 10.6, 2.7 Hz, 1H), 7.32 (ddd, *J* = 9.2, 8.3, 2.7 Hz, 1H), 6.64 (s, 1H), 3.95 (s, 3H), 3.89 (s, 3H), 2.48 (s, 3H). ^{13}C {^{1}H} NMR ($CDCl_3$, 101 MHz): δ 161.6, 159.1, 150.9 (d, *J* = 5.1 Hz), 147.1 (d, *J* = 1.4 Hz), 126.1 (d, *J* = 8.8 Hz), 125.7 (d, *J* = 0.8 Hz), 124.8 (d, *J* = 2.5 Hz), 124.2 (d, *J* = 8.7 Hz), 116.3 (d, *J* = 25.2 Hz), 106.3 (d, *J* = 22.5 Hz), 61.2, 55.5, 16.0. ^{19}F NMR ($CDCl_3$, 377 MHz): δ -116.24 (ddd, *J* = 10.3, 8.4, 5.5 Hz). HRMS (ESI) calcd for $C_{13}H_{14}FO_2$: 221.0972. Found 221.0971 ($M+H^+$).

(4-bromophenyl)(7-fluoro-1,4-dimethoxy-3-methylnaphthalen-2-yl)methanone 12. Compound **11** (1.5 g, 6.8 mmol, 1 equiv.) and 4-bromobenzoic acid (2 g, 10.2 mmol, 1.5 equiv.) were dissolved in dichloromethane (68 mL). At 0 °C, TFAA (1.9 mL, 13.6 mmol, 2 equiv.) was added. After stirring for 10 min, TfOH (0.3 mL, 3.4 mmol, 0.5 equiv.) was cautiously added and the reaction mixture was allowed to warm up slowly to room temperature and stirred for 16 h. Then, the reaction was quenched with an aqueous saturated $NaHCO_3$ solution. The aqueous phase was extracted three times with dichloromethane, dried with anhydrous magnesium sulfate and solvent was removed under vacuum. The crude was purified by silica gel chromatography (CHX/T, 2/8, v/v, UV, Rf = 0.5) to afford the desired product **12** (1.7 g, 62.6%) as an orange oil. ^{1}H NMR (400 MHz, $CDCl_3$) δ 8.19 – 8.08 (m, 1H), 7.74 – 7.69 (m, 2H), 7.65 (ddd, *J* = 10.0, 2.6, 0.6 Hz, 1H), 7.62 – 7.55 (m, 2H), 7.35 (ddd, *J* = 9.2, 8.2, 2.6 Hz, 1H), 3.90 (s, 3H), 3.78 (s, 3H), 2.20 (s, 3H). ^{19}F {^{1}H} NMR (377 MHz, $CDCl_3$) δ -113.55. ^{13}C {^{1}H} NMR (101 MHz, $CDCl_3$) δ 196.2, 162.5, 160.1, 150.8 (d, *J* = 1.5 Hz), 148.7 (d, *J* = 5.4 Hz), 135.9, 132.3, 131.8, 131.1, 129.4, 128.3 (d, *J* = 8.7 Hz), 126.6, 125.5 (d, *J* = 8.8 Hz), 122.9 (d, *J* = 2.5 Hz), 117.6 (d,

J = 25.4 Hz), 106.6 (d, *J* = 22.5 Hz), 63.6, 61.8, 12.8. HRMS (ESI) calcd. for $C_{20}H_{17}BrFO_3$: 403.0340. Found: 403.0326 ($M+H^+$).

(7-fluoro-1,4-dimethoxy-3-methylnaphthalen-2-yl)(4-((trimethylsilyl)ethynyl)phenyl)methanone 13. Compound **12** (682.1 mg, 1.7 mmol, 1 equiv.) was dissolved under argon in triethylamine (42.3 mL) in a dry double necked round bottom flask at room temperature. Then, $Pd(PPh_3)_2(Cl)_2$ (71.2 mg, 0.1 mmol, 0.06 equiv.), CuI (32.2 mg, 0.2 mmol, 0.1 equiv.) were added under argon and three cycles argon vacuum were performed, finally trimethylsilylacetylene (0.7 mL, 5.1 mmol, 3 equiv.) was added. The round bottom flask was stirred at 70 °C for 20 h. The reaction mixture was quenched with a 1/1 brine/water mixture and the aqueous phase was extracted three times with ethyl acetate, dried with anhydrous magnesium sulfate and solvent was removed under vacuum. The crude was purified by silica gel chromatography (CHX/EtOAc, 9/1, v/v, UV, Rf = 0.7) to afford the desired product **13** as a yellow oil quantitatively. ^{1}H NMR (400 MHz, $CDCl_3$) *δ* 8.13 (dd, *J* = 9.2, 5.5 Hz, 1H), 7.80 – 7.74 (m, 2H), 7.65 (dd, *J* = 10.0, 2.6 Hz, 1H), 7.53 – 7.50 (m, 2H), 7.34 (ddd, *J* = 9.3, 8.3, 2.6 Hz, 1H), 3.89 (s, 3H), 3.77 (s, 3H), 2.18 (s, 3H), 0.25 (s, 9H). ^{19}F {^{1}H} NMR (377 MHz, $CDCl_3$) *δ* -113.73. ^{13}C {^{1}H} NMR (101 MHz, $CDCl_3$) *δ* 196.5, 162.5, 160.1, 150.8, 148.7 (d, *J* = 5.3 Hz), 136.5, 132.4, 132.1, 129.5, 128.9, 128.4 (d, *J* = 8.8 Hz), 126.6, 125.8 (d, *J* = 8.9 Hz), 122.9 (d, *J* = 2.5 Hz), 117.6 (d, *J* = 25.4 Hz), 106.6 (d, *J* = 22.5 Hz), 88.1, 86.1, 63.5, 61.8, 12.8, -0.06. HRMS (ESI) calcd. for $C_{25}H_{26}FO_3Si$: 421.1630. Found: 421.1623 ($M+H^+$).

(4-ethynylphenyl)(7-fluoro-1,4-dimethoxy-3-methylnaphthalen-2-yl)methanone 14. To a solution of compound **13** (930 mg, 2.2 mmol, 1 equiv.) in THF (43 mL) was added at room temperature another solution of TBAF (1M in THF) (6.6 mL, 6.6 mmol, 3 equiv.). The crude mixture was stirred for 3 h and then the reaction was hydrolyzed with saturated aqueous ammonium chloride. The aqueous phase was extracted three times with ethyl acetate, dried with anhydrous magnesium sulfate and solvent was removed under vacuum. The crude was purified by silica gel chromatography (CHX/EtOAc, 10/0 to 9/1, v/v, UV, Rf = 0.7) to afford the desired product **14** as a yellow solid (522.4 mg, 67.8%). M.p. 121-123 °C. ^{1}H NMR (400 MHz, $CDCl_3$) *δ* 8.14 (dd, *J* = 9.2, 5.4 Hz, 1H), 7.82 – 7.76 (m, 2H), 7.65 (ddd, *J* = 10.0, 2.6, 0.5 Hz, 1H), 7.59 – 7.52 (m, 2H), 7.35 (ddd, *J* = 9.2, 8.3, 2.6 Hz, 1H), 3.90 (s, 3H), 3.78 (s, 3H), 3.26 (s, 1H), 2.19 (s, 3H). ^{19}F {^{1}H} NMR (377 MHz, $CDCl_3$) *δ* -113.65. ^{13}C {^{1}H} NMR (101 MHz, $CDCl_3$) *δ* 196.5, 162.5, 160.1, 150.8 (d, *J* = 1.7 Hz), 148.7 (d, *J* = 5.2 Hz), 136.9, 132.6, 132.0, 129.5, 128.4 (d, *J* = 8.8 Hz), 127.8, 126.6, 125.5 (d, *J* = 8.9 Hz), 122.9 (d, *J* = 2.6 Hz), 117.6 (d, *J* = 25.4 Hz), 106.6 (d, *J* = 22.5 Hz), 82.9, 80.9, 63.6, 61.8, 27.1, 12.8. HRMS (ESI) calcd. for $C_{22}H_{18}FO_3$: 349.1234. Found: 349.1225 ($M+H^+$).

3-(4-ethynylbenzoyl)-6-fluoro-2-methylnaphthalene-1,4-dione 3. Compound **14** (135 mg, 0.4 mmol, 1 equiv.) was dissolved in acetonitrile (4.6 mL), then under stirring CAN (467.4 mg, 0.8 mmol, 2.2 equiv.) dissolved in water (1.6 mL) was added. The reaction mixture was stirred for 1 h. Once the reaction was complete, acetonitrile was removed under vacuum and the aqueous phase was extracted three times with dichloromethane, dried with anhydrous magnesium sulfate and solvent was removed under vacuum (CHX/EtOAc, 9/1, v/v, UV, Rf = 0.3). The desired product **3** was obtained as a yellow solid (116 mg, 94%). M.p. 142-144 °C. ^{1}H NMR (400 MHz, $CDCl_3$) *δ* 8.22 (dd, *J* = 8.6, 5.2 Hz, 1H), 7.88 – 7.81 (m, 2H), 7.71 (dd, *J* = 8.3, 2.6 Hz, 1H), 7.63 – 7.57 (m, 2H), 7.51 – 7.41 (m, 1H), 3.30 (s, 1H), 2.07 (s, 3H). ^{19}F {^{1}H} NMR (377 MHz, $CDCl_3$) *δ* -100.79. ^{13}C NMR (101 MHz, $CDCl_3$) *δ* 192.6, 183.5, 182.3, 167.7, 165.1, 144.8, 144.2, 135.3, 134.3 (d, *J* = 8.0 Hz), 132.9, 130.3 (d, *J* = 9.0 Hz), 129.1, 128.7, 128.7 (d, *J* = 4.0 Hz), 121.6 (d, *J* = 22.6 Hz), 113.3 (d, *J* = 23.5 Hz), 82.6, 81.6, 13.8. HRMS (ESI) calcd. for $C_{20}H_{12}FO_3$: 319.0765. Found: 319.0758 ($M+H^+$).

Synthesis of probe 5

6-fluoro-3-(4-iodobenzyl)-2-methylnaphthalene-1,4-dione 19. 6-fluoro-menadione (250 mg, 1.3 mmol, 1 equiv.) and 2-(4-iodophenyl)acetic acid (689 mg, 2.6 mmol, 2 equiv.) were dissolved in a mixture of acetonitrile (20 mL) water (7 mL). Then $AgNO_3$ (78.2 mg, 0.5 mmol, 0.35 equiv.) and ammonium persulfate (390 mg, 1.7 mmol, 1.3 equiv.) was added in the reaction mixture. The reaction was stirred for 4 h at 85 °C in the dark. The solvent was removed in vacuum and then extracted three times with ethyl acetate. Reunited organic layers were washed with water, dried with anhydrous magnesium sulfate, filtered and the solvent was removed under reduced pressure. The crude was purified by silica

gel chromatography (CHX/DCM, 5/5, v/v, UV, Rf = 0.7) to afford the desired product **19** quantitatively as a yellow solid. M.p. 91-93 °C. ^{1}H NMR (400 MHz, $CDCl_3$) δ 8.13 (dd, J = 8.6, 5.3 Hz, 1H), 7.72 (dd, J = 8.6, 2.7 Hz, 1H), 7.61 – 7.57 (m, 2H), 7.36 (ddd, J = 8.6, 8.0, 2.7 Hz, 1H), 7.01 – 6.93 (m, 2H), 3.96 (s, 2H), 2.24 (s, 3H). ^{19}F {^{1}H} NMR (377 MHz, $CDCl_3$) δ -102.31. ^{13}C {^{1}H} NMR (126 MHz, $CDCl_3$) δ 183.9, 183.5, 167.1, 165.1, 144.9 (d, J = 1.7 Hz), 138.5, 137.8, 134.6 (d, J = 7.8 Hz), 132.7, 130.9, 130.7, 129.7 (d, J = 8.7 Hz), 128.8 (d, J = 3.2 Hz), 120.9 (d, J = 22.5 Hz), 113.3 (d, J = 23.4 Hz), 91.9, 32.2, 13.5. HRMS (ESI) calcd. for $C_{18}H_{13}FIO_2$: 406.9939. Found: 406.9922 ($M+H^+$).

6-fluoro-3-(4-iodobenzyl)-1,4-dimethoxy-2-methylnaphthalene 20. Compound **19** (550 mg, 1.3 mmol, 1 equiv.), was solubilized in MeOH (5.1 mL) then a solution of tin chloride (642 mg, 3.4 mmol, 2.5 equiv.) in 37% aqueous HCl (0.5 mL, 5.6 mmol, 4.12 equiv.) was added dropwise and the mixture was stirred 30 min at room temperature until the solution came back yellowish. Most of the solvent was evaporated under vacuum, the yellow precipitate was rinsed with water. The powder was dissolved in acetone (5.1 mL) and dried with anhydrous magnesium sulfate. Under argon, dimethyl sulfate (0.6 mL, 6.8 mmol, 5 equiv.) was added to the previous mixture then a solution of KOH (379.8 mg, 6.8 mmol, 5 equiv.) in MeOH (1.3 mL) was added drop by drop. When the addition was completed the mixture was stirred at reflux 60 °C during 1 h. A 20% aqueous solution of KOH (10 mL) was added to the mixture and organic solvent were removed under vacuum. The aqueous phase was extracted three times with dichloromethane, dried with anhydrous magnesium sulfate and solvent was removed under vacuum (CHX/T, 2/8, v/v, UV, Rf = 0.4). The crude residue gave the desired product **20** (426 mg, 72.1%) as an orange oil. ^{1}H NMR (400 MHz, $CDCl_3$) δ 7.99 (dd, J = 9.3, 5.6 Hz, 1H), 7.58 (ddd, J = 10.4, 2.6, 0.5 Hz, 1H), 7.47 – 7.40 (m, 2H), 7.17 (ddd, J = 9.1, 8.3, 2.7 Hz, 1H), 6.80 – 6.69 (m, 2H), 4.10 (s, 2H), 3.75 (s, 3H), 3.71 (s, 3H), 2.12 (s, 3H). ^{19}F {^{1}H} NMR (377 MHz, $CDCl_3$) δ -114.71. ^{13}C {^{1}H} NMR δ 162.0, 160.1, 150.7, 150.2 (d, J = 5.3 Hz), 140.0, 137.8, 137.6, 130.3, 130.1, 128.3 (d, J = 8.5 Hz), 126.1 (d, J = 2.5 Hz), 125.2, 125.1, 116.2 (d, J = 25.3 Hz), 106.3 (d, J = 22.3 Hz), 91.1, 62.3, 61.7, 32.5, 12.7. HRMS (ESI) calcd. for $C_{20}H_{19}FIO_2$: 437.0408. Found: 437.0409 ($M+H^+$).

((4-((7-fluoro-1,4-dimethoxy-3-methylnaphthalen-2-yl)methyl)phenyl)ethynyl)trimethylsilane 21. Compound **20** (426 mg, 1 mmol, 1 equiv.) was dissolved under argon in triethylamine (24.4 mL) in a dry double necked round bottom flask at room temperature. Then, $Pd(PPh_3)_2(Cl)_2$ (41 mg, 0.06 mmol, 0.06 equiv.), CuI (18.6 mg, 0.1 mmol, 0.1 equiv.) were added under argon and three cycles argon vacuum were performed, finally trimethylsilylacetylene (0.4 mL, 2.9 mmol, 3 equiv.) was added. The round bottom flask was stirred at 70 °C for 24 h. The reaction mixture was quenched with a 1/1 brine/water mixture and the aqueous phase was extracted three times with ethyl acetate, dried with anhydrous magnesium sulfate and solvent was removed under vacuum (CHX/T, 2/8, v/v, UV, Rf = 0.6). The crude residue gives the desired product **21** quantitatively as a brown oil. ^{1}H NMR (500 MHz, $CDCl_3$) δ 8.08 (dd, J = 9.2, 5.6 Hz, 1H), 7.69 – 7.64 (m, 1H), 7.36 – 7.32 (m, 2H), 7.29 – 7.23 (m, 2H), 7.03 (dt, J = 8.7, 0.8 Hz, 2H), 4.24 (s, 2H), 3.83 (s, 3H), 3.78 (s, 3H), 2.19 (s, 3H), 0.22 (s, 9H). ^{19}F {^{1}H} NMR (377 MHz, $CDCl_3$) δ -114.88. ^{13}C {^{1}H} NMR (126 MHz, $CDCl_3$) δ 162.1, 160.1, 150.7, 150.2 (d, J = 5.3 Hz), 141.1, 132.2, 132.2, 131.7 (d, J = 8.0 Hz), 130.3, 129.6 (d, J = 7.4 Hz), 128.1, 126.3 (d, J = 2.3 Hz), 125.2 (d, J = 9.1 Hz), 120.8, 116.2 (d, J = 25.4 Hz), 106.4 (d, J = 22.3 Hz), 105.2, 93.8, 62.3, 61.7, 32.9, 12.7, 0.1. HRMS (ESI) calcd. for $C_{25}H_{28}FO_2Si$: 407.1837. Found: 407.1808 ($M+H^+$).

3-(4-ethynylbenzyl)-6-fluoro-1,4-dimethoxy-2-methylnaphthalene 22. To a solution of compound **21** (470 mg, 1.2 mmol, 1 equiv.) in THF (22.5 mL) was added at room temperature another solution of TBAF trihydrate (1.1 g, 3.5 mmol, 3 equiv.) in THF (11.2 mL). The crude mixture was stirred for 3 h and then the reaction was hydrolyzed with saturated aqueous ammonium chloride. The aqueous phase was extracted three times with ethyl acetate, dried with anhydrous magnesium sulfate and solvent was removed under vacuum (CHX/T, 2/8, v/v, UV, Rf = 0.5). The crude residue gives the desired product **22** quantitatively as a brown oil. ^{1}H NMR (500 MHz, $CDCl_3$) δ 8.08 (dd, J = 9.2, 5.6 Hz, 1H), 7.67 (dd, J = 10.4, 2.6 Hz, 1H), 7.37 (d, J = 8.3 Hz, 2H), 7.29 – 7.23 (m, 1H), 7.06 (d, J = 7.7 Hz, 2H), 4.25 (s, 2H), 3.84 (s, 3H), 3.80 (s, 3H), 3.02 (s, 1H), 2.21 (s, 3H). ^{19}F {^{1}H} NMR (377 MHz, $CDCl_3$) δ -114.85. ^{13}C {^{1}H} NMR (126 MHz, $CDCl_3$) δ 162.1, 160.1, 150.8, 150.3 (d, J = 5.3 Hz), 141.4, 132.4 (d, J = 8.0 Hz), 130.2, 128.4 (d, J = 7.4 Hz), 128.2, 126.2 (d, J = 2.3 Hz), 125.3 (d, J = 9.1 Hz), 119.8, 116.3 (d, J = 25.4 Hz), 106.5 (d, J = 22.3 Hz), 83.8, 62.3, 61.7, 32.9, 12.7. HRMS (ESI) calcd. for $C_{22}H_{19}O_2F_{23}Na$: 357.1261. Found: 357.1258 ($M+Na^+$).

3-(4-ethynylbenzyl)-6-fluoro-2-methylnaphthalene-1,4-dione 5. Compound **22** (404 mg, 1.2 mmol, 1 equiv.) was dissolved in acetonitrile (14.5 mL), then under stirring CAN (1.5 g, 2.7 mmol, 2.2 equiv.) dissolved in water (4.8 mL) was added. The reaction mixture was stirred for 1 h. Once the reaction was complete, acetonitrile was removed under vacuum and the aqueous phase was extracted three times with dichloromethane, dried with anhydrous magnesium sulfate and solvent was removed under vacuum (CHX/EtOAc, 9/1, v/v, UV, Rf = 0.3). The crude residue gives the desired product **5** quantitatively (287.6 mg, 78%) as an orange solid. M.p. 102-104 °C. ^{1}H NMR (500 MHz, $CDCl_3$) δ 8.13 (dd, J = 8.6, 5.2 Hz, 1H), 7.73 (dd, J = 8.6, 2.6 Hz, 1H), 7.41 – 7.33 (m, 3H), 7.19 – 7.13 (m, 2H), 4.02 (s, 2H), 3.03 (s, 1H), 2.24 (s, 3H). ^{19}F {^{1}H} NMR (377 MHz, $CDCl_3$) δ -102.37.^{13}C {^{1}H} NMR (126 MHz, $CDCl_3$) δ 184.1, 183.6, 167.2, 165.1, 145.1 (d, J = 3.1 Hz), 138.9, 134.7 (d, J = 7.8 Hz), 132.6, 129.8 (d, J = 8.7 Hz), 128.8 (d, J = 3.3 Hz), 128.7, 121.0, 120.8, 120.5, 113.5, 113.3, 83.5, 77.3 (d, J = 9.3 Hz), 32.6, 13.5. HRMS (ESI) calcd. for $C_{20}H_{13}O_2F_{23}Na$: 327.0792. Found: 327.0792 ($M+Na^+$).

B1.3. Synthesis of 6-fluoro-PDO

6-fluoro-2-methyl-3-(4-(trifluoromethyl)benzyl)naphthalene-1,4-dione 6-fluoro-PD (Cpd **17e** in [32])**.** 6-fluoro-menadione (500 mg, 2.6 mmol, 1 equiv.) and 4-(trifluoromethyl)phenylacetic acid (1 g, 5.3 mmol, 2 equiv.) were dissolved in acetonitrile (40 mL) and water (13.5 mL). The mixture was heated to 85 °C and silver nitrate (156.3 mg, 0.9 mmol, 0.35 equiv.) with ammonium persulfate (780 mg, 3.4 mmol, 1.3 equiv.) were added. The reaction was stirred for 4 h at 85 °C in the dark. The solvent was removed in vacuum and then extracted three times with ethyl acetate. Reunited organic layers were washed with water, dried over magnesium sulfate, filtered and the solvent was removed under reduced pressure (CHX/EtOAc, 8/2, v/v, UV, Rf = 0.4). The crude, mainly containing **6-fluoro-PD** as an orange oil, was directly engaged in the next reaction without purification.

6-fluoro-2-methyl-3-(4-(trifluoromethyl)benzoyl)naphthalene-1,4-dione (6-fluoro-PDO). In a tube was dissolved in a mixture of propan-2-ol (1.3 mL) and DCM (1.7 mL), **6-fluoro-PD**[32] (100 mg, 0.3 mmol, 1 equiv.), then the mixture was stirred 72h under dioxygen at 16 °C under UV irradiation. Solvents were removed under reduced pressure and the crude was purified by silica gel chromatography (CHX/DCM, 5/5, v/v, UV, Rf = 0.3) to afford **6-fluoro-PDO** as a yellow solid (38.5 mg, 37%). M.p. 155-157 °C. ^{1}H NMR (400 MHz, $CDCl_3$) δ 8.23 (dd, J = 8.6, 5.2 Hz, 1H), 8.01 (d, J = 7.8 Hz, 2H), 7.77 (d, J = 8.2 Hz, 2H), 7.70 (dd, J = 8.3, 2.6 Hz, 1H), 7.47 (td, J = 8.3, 2.7 Hz, 1H), 2.08 (s, 3H). ^{19}F {^{1}H} NMR (377 MHz, $CDCl_3$) δ -63.31, -100.54. ^{13}C {^{1}H} NMR (101 MHz, $CDCl_3$) δ 192.6, 183.3, 182.4 (d, J = 1.7 Hz), 167.7, 165.2, 145.2, 143.8 (d, J = 1.9 Hz), 138.3, 135.8 (q, J = 32.8 Hz), 134.2 (d, J = 8.0 Hz), 130.3, 129.5, 128.6 (d, J = 3.7 Hz), 126.4 (q, J = 3.8 Hz), 123.5 (q, J = 272.9 Hz), 121.8 (d, J = 22.5 Hz), 113.4 (d, J = 23.6 Hz), 27.0, 13.8. HRMS (ESI) calcd. for $C_{19}H_{11}F_4O_3$: 363.0639. Found: 363.0635 ($M+H^+$).

B2. Characterization Techniques

B2.1. Characterization of the photo-crosslinked and probe-reacted protein adducts

B2.1.1. Revelation of the ABPP probe-glutathione reductase adduct upon click reaction with rhodamine azide by fluorescence

During photoaffinity labeling of recombinant proteins with ABPP probes **1** and **2**,[19] we observed a green fluorescence associated to the photo-irradiated probe-protein adduct in SDS-PAGE, independent of the click product with rhodamine azide, when the non “clickable” **PDO** was added (Figure S1). A decreased fluorescence associated to the alkylated protein band was expected in the presence of the competitor **PDO**. Instead, we observed an increase of the fluorescence associated to the **PDO**-protein adduct in gels, but not to the probes **1** or **2**-protein adducts alone. The comprehensive understanding of this fluorescence was recently made.[23] Indeed, we demonstrated that the reduced and thiol-alkylated species II, the “open” probe adduct derived from **PDO** or **F-PDO** (see structure of **F-PDO** in the Scheme of Figure S3) exhibited emission properties in the visible region, due to a keto-enol tautomerization,

making them valuable fluorescent probes to monitor protein alkylation processes, and also the redox status within living cells such as BY-2 tobacco cells. These emission properties are closely related to the ability of benzoylMDs with a -CF_3 group in *para* to generate a fluorescent alkylated reduced species under (photo)-reduction through an Excited State Intramolecular Photoinduced Transfer (ESIPT) mechanism with a very large Stokes gap of about 95 nm and a characteristic bright yellowish emission, as recently reported.[23]

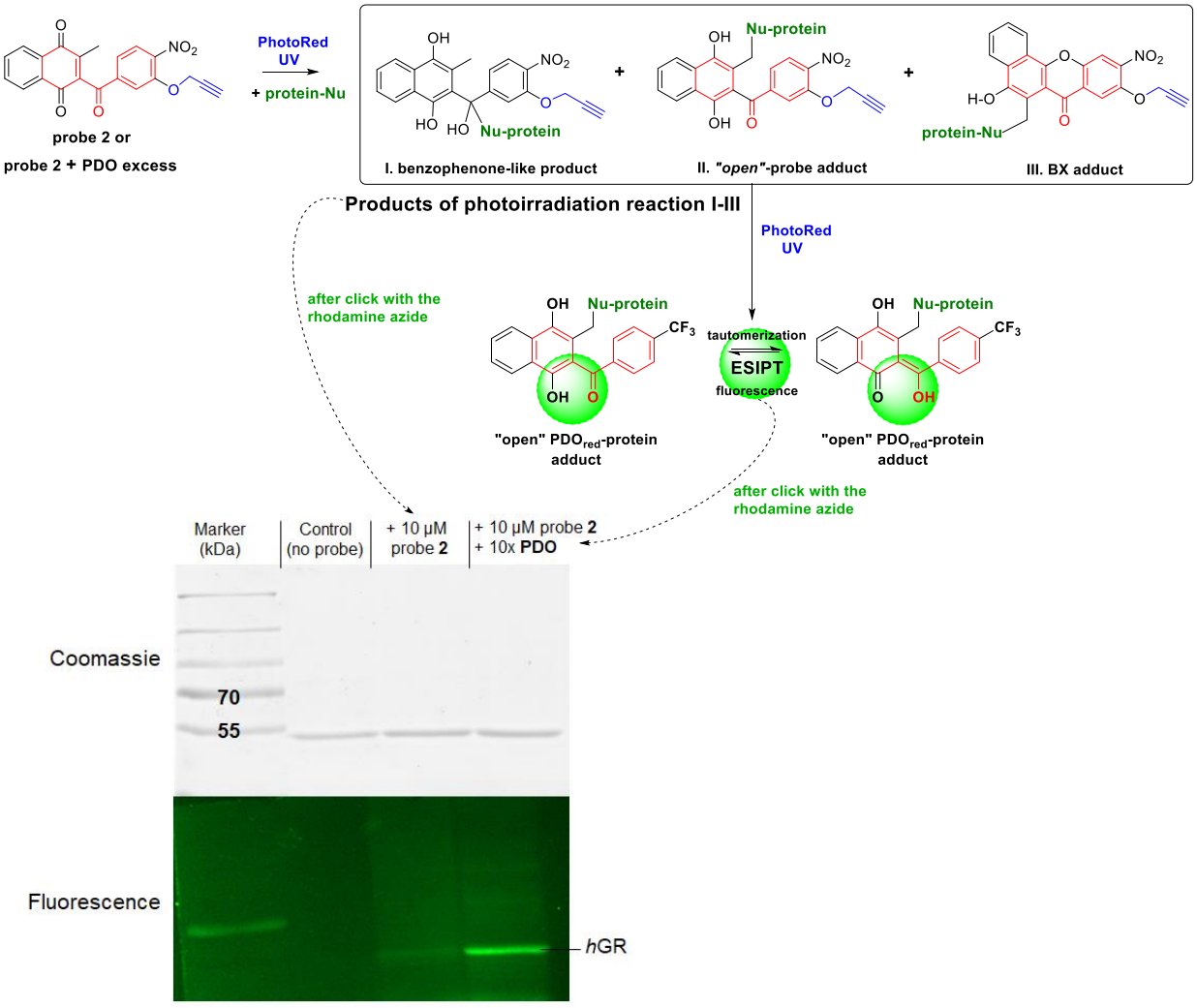

Figure S1. Photoaffinity labeling of *h*GR with the ABPP probe **2** and clicked with rhodamine azide. Scheme shows the three previously described photoirradiation products (box). UV-irradiation of the *h*GR in the presence of probe **2** led to three distinct photoirradiation products (I-II-III).

Figure of the SDS-Page gel stained with Coomassie (top) is pictured. Below: For each click reaction with rhodamine azide (no probe, probe **2**, probe **2** + 10 equiv. **PDO**), the reaction mixtures were loaded on the gel. *h*GR is localized at the height of the 55 kDa marker band. When the experiment is performed in the presence of an excess of **PDO**, a more intense fluorescent signal was observed in the SDS-PAGE gel. The fluorescence increase is due to an ESIPT-generated fluorescence in the presence of the tautomeric β-keto-enol form of the **PDO$_{red}$**-*h*GR protein adduct (species II, “open” probe adduct with **PDO**).

B2.1.2. Revelation of the PDO-BSA adducts by ESIPT fluorescence

Therefore, we tested whether the emission generated during the reaction could belong to an adduct formed between the photo-reduced naphthoquinone and the protein containing a nucleophilic function, e.g. a thiol. As an example, we incubated either **BX** (i.e. the benzoxanthone **BX** is a putative **PDO** metabolite resulting from oxidative phenolic coupling reaction from the reduced **PDO** radical, Figure 1 Panel A), or **PDO**, and analyzed the appearance of fluorescently labeled proteins by gel electrophoresis (Figure S2). Although **BX** only weakly labels BSA independent of oxygen conditions, **PDO** generates a strong green fluorescent signal associated to BSA in comparison. This demonstrates that a covalent bond between the two compounds is most likely the source of the observed fluorescence emission.

Figure S2. BSA photolabeling with **PDO** in the absence of rhodamine azide. 100 µM of **BX** or **PDO** were incubated with a mixture of 5 µM of protein and UV-irradiated at 350 nm under the oxygen (Ox) conditions indicated for **BX** for 10 min and for **PDO** for 1.5 h (10% DMSO solvent concentration in 47mM potassium phosphate buffer). Then, the samples were mixed with loading buffer and subjected to SDS-PAGE. Upper panel - fluorescence gel visualization, lower panel - Coomassie staining.

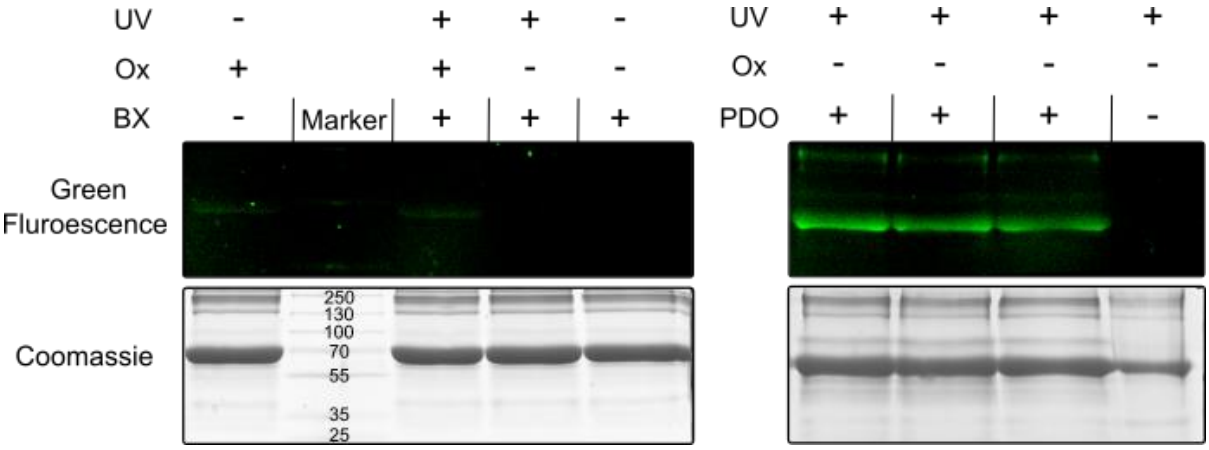

B2.1.3. Revelation of the PDO-protein adduct by ESIPT fluorescence spectra

An exploration study was made to investigate if the observed fluorescence could be exploited with several pure recombinant proteins (Figure S3). Our data suggest that covalent labeling of proteins necessitates a certain amount of solvent-exposed cysteine/nucleophile to react. Indeed, the labeling is i) catalyzed by oxidoreductases as the signal is strongest upon reaction with *h*GR or *Pf*FNR, and more limited with BSA; ii) is most likely dependent on the amount of free cysteines/nucleophiles as the addition of BSA to *h*GR further increased the fluorescence signal; iii) a proximity labeling as BSA labeling was most likely catalyzed by *h*GR. We concluded that the ESIPT fluorescence could not be an effective method to detect probe-protein adducts from reactions with complex protein mixtures in an ABPP strategy as it was dependent on the protein cysteine amount that may vary between samples.

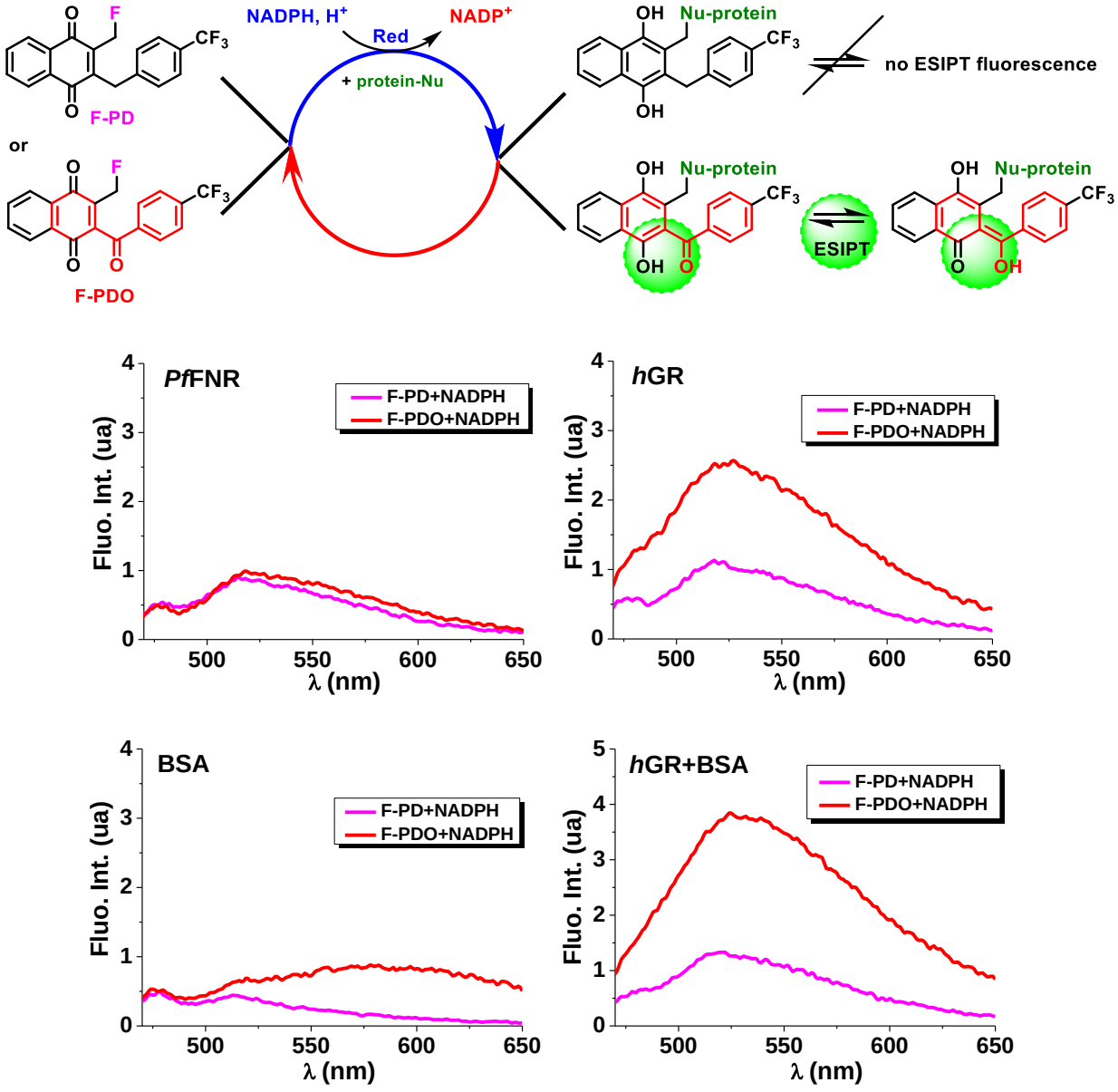

Figure S3. Scheme of the enzymatic redox-cycling and emission spectra recorded for the benz(o)ylMD **F-PDO**, **F-PD** after 30 min reaction with 2x addition of 200 µM NADPH in the presence of the proteins *Pf*FNR, BSA, *h*GR or *h*GR+BSA. [bMD] = 40 µM; [Protein] = 40 µM. Solvent: water/DMSO (7/3 v/v) buffered at pH 6.9; λ_{exc} = 440 nm.

B2.1.4. Revelation of the probe-thiol adduct by ESIPT fluorescence spectra

Of note, the observed ESIPT fluorescence was the strongest with **F-PDO** as compared to **PDO**, both of them having a -CF_3 group in *para* position at the benzylic chain, while there is almost no fluorescence associated to the probe-thiol adducts when this position is occupied by a -NO_2 group, as in the non-clickable probe **6** (Figure S4).

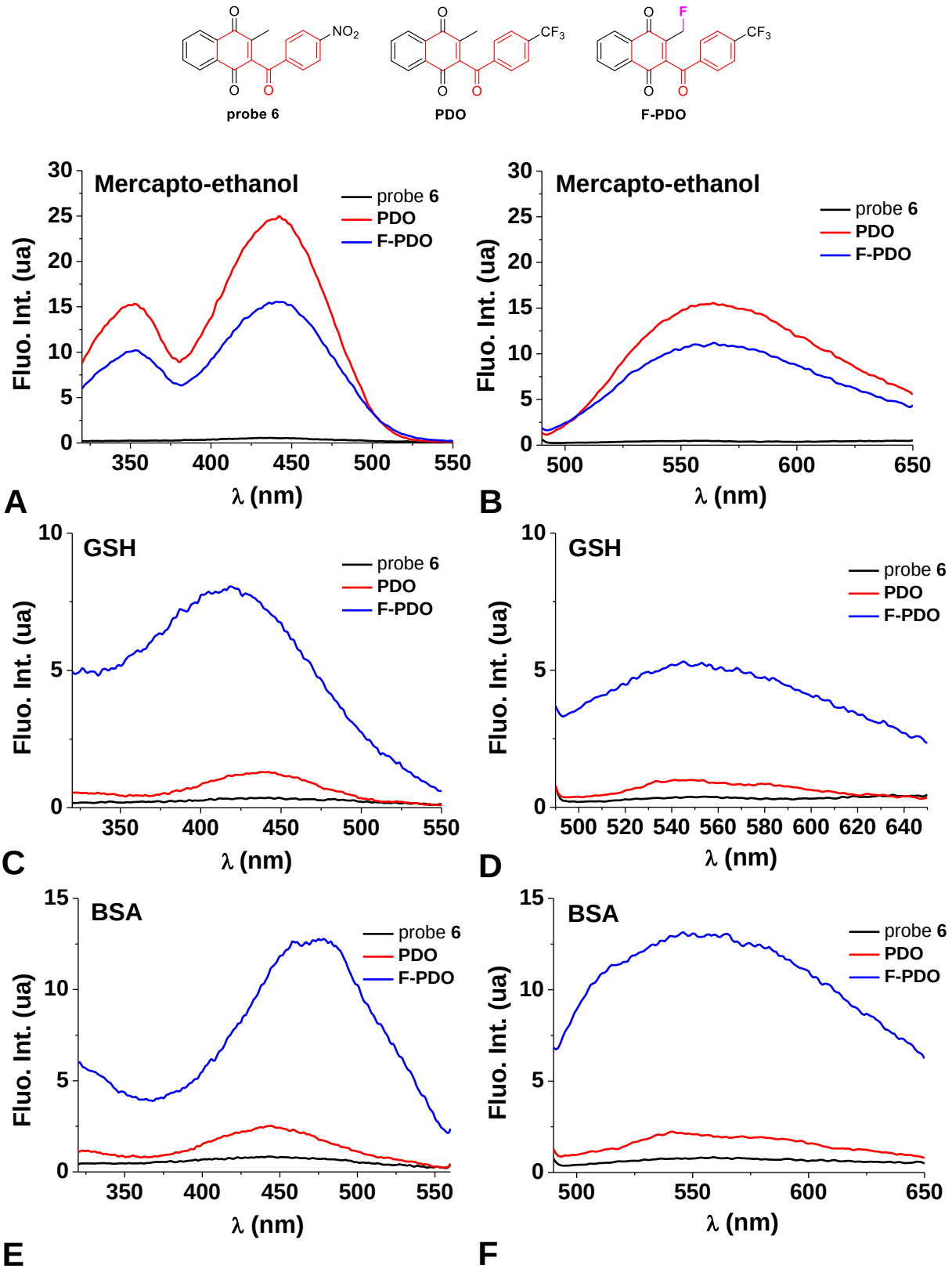

Figure S4. Fluorescence associated to the UV-irradiated benzoylMD-thiol adducts: Excitation (left panels A,C,E) and emission (right panels B, D, F)) spectra recorded for the benzoylMD **6**, **PDO** and **F-PDO** after irradiation at 350 nm (Rayonet photochemical reactor equipped with 16 UV lamps of 14 W and maintained at 16 °C) for 2 h under air atmosphere in the presence of various thiols. [**benzoylMD**] = 40 µM; [β-met] = 40 µM; or [GSH] = 40 µM or [BSA] = 40 µM. Solvent: H_2O/DMSO (7:3 *v/v*) buffered at pH 6.9; λ_{exc} = 470 nm.

B2.2. Optimization of the click reaction with probes 1 - 3

For the optimization of the CuAAC reaction yield using probe **1** and biotin azide (BA), we tested several conditions in terms of catalyst type and concentration, temperature and solvent, as reported in Table S1. The presence of the click product from the reaction between probe 1 was confirmed by LC-MS analysis where a chromatographic peak corresponding to the species *m/z* 701.2740 was detected (Figure S7, chromatogram A). For each condition, we monitored the click product concentration and the reactant consumption in a time-course manner by measuring the chromatogram peak areas; and the yield of reaction was obtained using the extracted ion chromatogram (EIC) method.

When we compared the peak area of the click product in the conditions #1 and #3 of Table S1, we noticed that the abundance of the species generated in the presence of the Cu(I) complex catalyst was far greater than that with Cu(II) + TCEP reductant (Figure S5A). The abundance of the click product generated by Cu(II) + TCEP was at most 36% of that obtained by the Cu(I)-catalyzed reaction, indicating that Cu(I) complex better catalyzes the click-reaction as compared to Cu(II) in the presence of TCEP reductant. We also compared the influence of the solvent used to dissolve the probe (conditions #1 and #2 in Table 1, Figure 5B). The probe solution in acetonitrile (ACN) gave better results in terms of click product amount compared to the DMSO condition.

As displayed in the bar graph in Figure S5B, the probe solution in acetonitrile (ACN) gave better results in terms of click product amount compared to the DMSO condition.

Although the better conditions in terms of catalyst and solvent were applied (condition #1), yields never went beyond 15% (data not shown). Upon temperature increase (from 30°C to 56°C), we were able to shorten the reaction times from over-night incubation to 90 minutes (condition #4) and reached almost 35% of reaction yield (Figure 3). Deoxygenation of the reaction mixture through Argon insufflation [19] (condition #5) further increased the yield up to 85% after 90 minutes of reaction (Figure S6).

Table S1. Screening of the conditions used to test the efficiency of click reaction. ACN: acetonitrile; BA: biotin azide; BCDA: bathocuproinedisulfonic acid; TCEP: tris(2-carboxyethyl)phosphine. Cu(I) complex: tetrakis(acetonitrile)copper(I) tetrafluoroborate; Cu(II) + reductant: Copper sulfate + TCEP.

Conditions	[Probe 1] (µM)	BA (µM)	Solvent	Catalyst, molar ratio ([conc.])	Temperature (°C)	Reaction Times (min.)	Deoxygena-tion
1	**1**, 24	50	0.5% ACN in PBS	Cu(I):BCDA, 1:1 (300 µM)	30	120, 180, 300, 1200	-
2	**1**, 24	50	0.5% DMSO in PBS	Cu(I):BCDA, 1:1 (300 µM)	30	120, 180, 300, 1200	-
3	**1**, 24	50	0.5% ACN in PBS	$CuSO_4$: BCDA:TCEP, 5:1:1 (660: 132:132 µM)	30	120, 180, 300, 1200	-
4	**1**, 24	50	0.5% ACN in PBS	Cu(I):BCDA, 1:1 (300 µM)	56	30, 90, 130	-
5	**1**, 24	50	0.5% ACN in PBS	Cu(I):BCDA, 1:1 (300 µM)	56	30, 90, 130	+

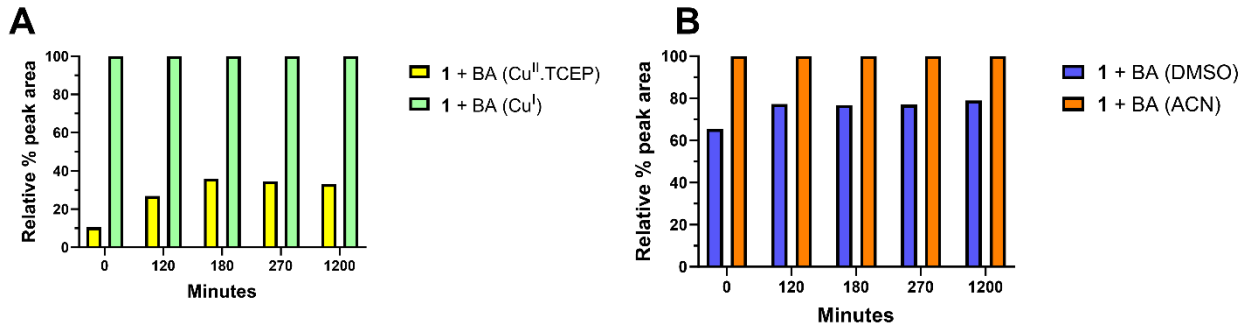

Figure S5. Formation of the click product between probe **1** and biotin azide (BA) as the function of time (panel A) in Cu(II) + TCEP *versus* Cu(I) complex, and (panel B) in ACN *versus* DMSO conditions. At each time point, 100% corresponds to the area of the most abundant species when the two tested conditions are compared.

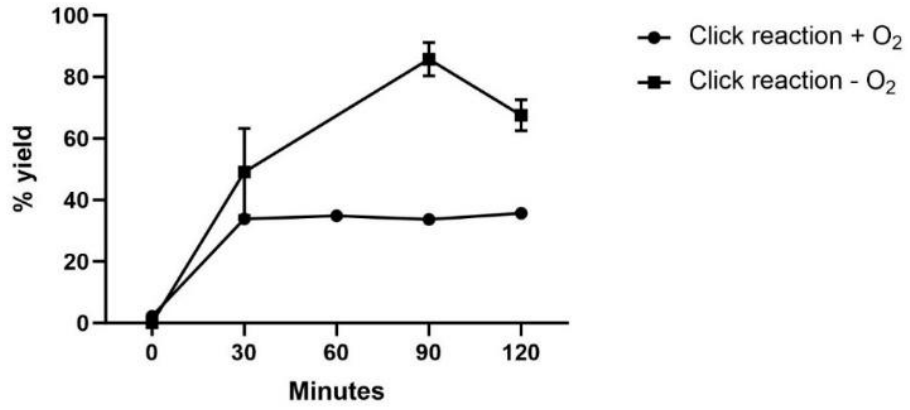

Figure S6. Yield (%) of the click product as the function of time in the presence or absence of dioxygen. The mean and standard error of the mean of three replicates are plotted. Conditions: "+O_2" means in open air. "-O_2" means that air was discarded by 8 cycles of argon/vacuum.

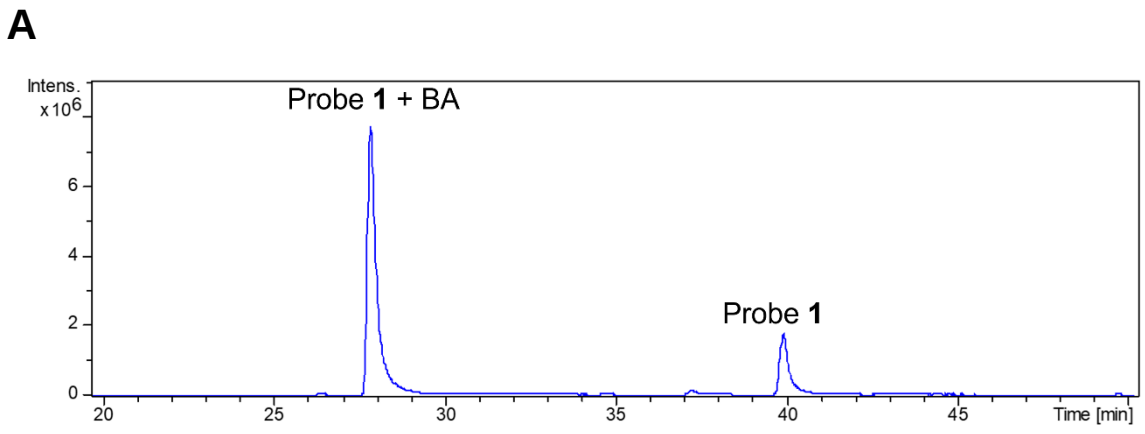

B

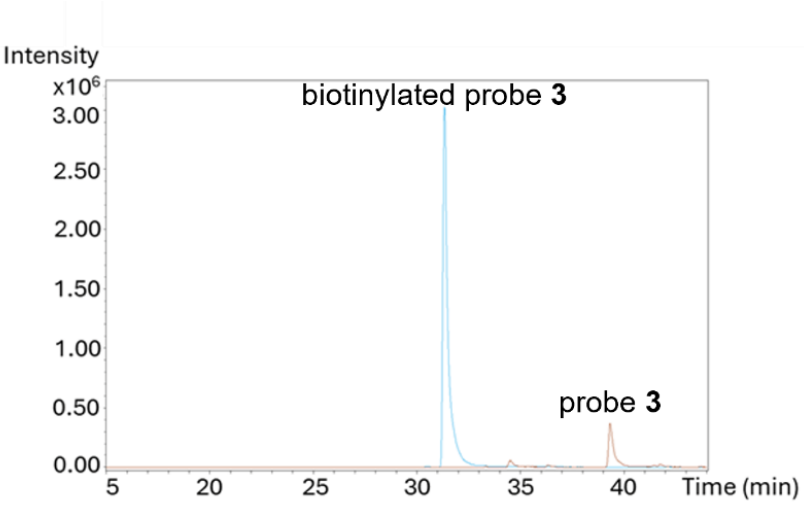

Figure S7. Panel A: Representative extracted ion chromatograms (EIC) of the ions with *m/z* 701.2740 ± 0.005 and 301.0856 ± 0.005 corresponding to MH+ values of the click product (probe **1** + BA) and the unreacted probe (probe **1**), respectively. The click product elutes at 28 min, whereas the probe **1** appears at 40 minutes in the chromatogram. Panel B: Extracted ion chromatograms (EIC) relative to the probe **3** and biotinylated probe after the click reaction, showing two ion peaks, respectively, for the probe **3** with a retention time of about 39.3 min (probe **3**, *m/z* 319.09) and the biotinylated probe **3** with a retention time of about 31.3 min (biotinylated **3**, *m/z* 719.27).

B2.3. Detection of the photo-crosslinked *Pf*GR and the protein-probe 2-adducts by Western-blot and Immunofluorescence

To evaluate the effectiveness of the AfBPP strategy with the optimized click reaction, we carried out an experiment using the recombinant *Pf*GR and the previously reported ABPP probe **2**.[19] The band corresponding to biotinylated *Pf*GR was observed in the presence of probe **2** and not in the control (no probe) after enrichment on streptavidin beads (Figure S8), and detection by α-biotin antibodies on Western-Blot membrane.

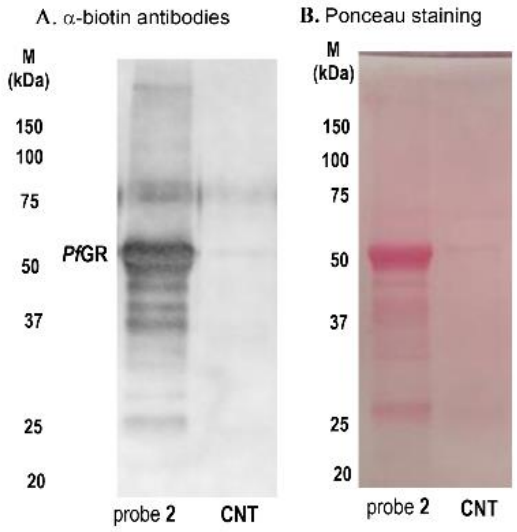

Figure S8. Western blot to reveal biotinylated proteins by immunofluorescence with α-biotin antibodies in the enriched recombinant *Pf*GR-probe adducts after AfBPP (Panel A) and Ponceau staining of the same membrane (Panel B). *Pf*GR: recombinant *Plasmodium falciparum* glutathione reductase. Recombinant *Pf*GR was subjected to the AfBPP strategy in the presence of probe **2** (probe **2** line) or in absence of any probe (**CNT**). Condition #5 was used for the click reaction (Table S1); 10 µL streptavidin beads for the pull down; beads binding buffer: 150 mM NaCl, 0.1% NP-40 in PBS; beads washing buffer: 300mM NaCl (1x), 0.1% SDS (2x), PBS (1x).

B2.4. Electrochemistry

In the benzylMD series, a first comparison of compound **4** and **PD** allowed us to assess the influence of the introduction of an alkyne vs -CF_3 function on the benzyl moiety in C-4' (*para*) (Table S2). While the first redox wave seems to be unaltered, a more significant effect can be observed on the second redox process leading to the dihydronaphthoquinone. The introduction of an alkyne function thus makes the reduction of semi-naphthoquinone to dihydronaphthoquinone more difficult. In the benzoylMD series, the replacement of the *para*-CF_3 by a *para*-alkyne moiety does not profoundly alter the redox properties of the naphthoquinone moiety. However, a difference of about 50 mV on the carbonyl reduction wave, between the alkyne and trifluoromethyl group substituted in C-4' of the benzoylMDs (**1** vs **PDO**) was indeed detected, attesting for a significant effect on redox properties centered on the carbonyl function. As expected, the electronic effect of fluorination at C-6 of the menadione moiety (**6-fluoro-PDO** vs **PDO**) is also significant. Indeed, such a substitution (electron-withdrawing effect of the fluorine atom) significantly modifies the two processes centered on the naphthoquinone moiety, making the systems more oxidant without altering the carbonyl function. While the voltammograms for the non-fluorinated compounds studied in this work do not show any processes other than those expected, the measurements carried out on the **6-fluoro-PDO** and compound **3** show more complex profiles, indicating parallel processes (e.g. degradation, dimerization, etc.). Compound **3**, characterized by the presence of a fluorine atom at C-6 of the menadione moiety and an alkyne function on its benzyl moiety, displays a very complex profile. The first redox process now appears to be irreversible, while the second appears to be quasi-reversible. Furthermore, these two combined substitutions favor the reduction of the semi-naphthoquinone and the carbonyl function. Other redox processes measured at more cathodic potentials can be observed suggesting side reactions.

Table S2. Electrochemical data measured using cyclic voltammetry (CV)[a] and Square Wave Voltammetry (SWV)[b]. Solvent: DMSO; *I* = 0.1 M $nNBu_4PF_6$, *v* = 200 mV s^{-1}. NA: not applicable.

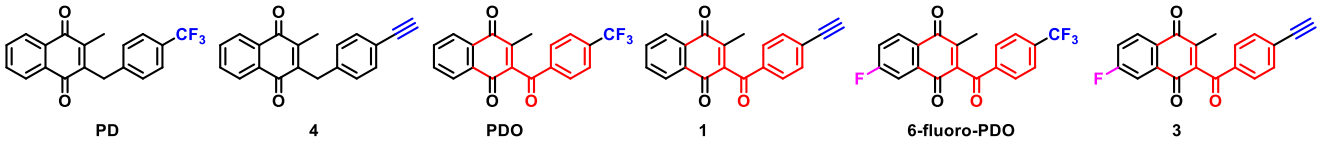

		Quinone		Carbonyl group
Series	**Compound**	**$E^1_{1/2}(\Delta E)^{[a]}/E^1_{1/2}{}^{[b]}$ [V(mV)][a]/[V][b]**	**$E^2_{1/2}(\Delta E)^{[a]}/E^2_{1/2}{}^{[b]}$ [V(mV)][a]/[V][b]**	**$E^3_{1/2}(\Delta E)^{[a]}/E^3_{1/2}{}^{[b]}$ [V(mV)][a]/[V][b]**
3-benzylmenadione	**PD**[17]	-0.59 (76)	-1.27 (78)	NA
	4	-0.60 (92) / -0.57	-1.24 (100) / -1.19	NA
3-benzoylmenadione	**PDO**	-0.43 (80)	-1.12 (84)	-1.62 (60)
	1	-0.44 (88) / -0.42	-1.15 (108) / -1.14	-1.56 (116) / -1.54
	6-fluoro-PDO	-0.37 (74) / -0.35	-1.09 (76) / -1.07	-1.55
	3	-0.45	-1.05	-1.50

Solvent: DMSO; *I* = 0.1 M $nNBu_4PF_6$, *v* = 200 mV s^{-1}. NA: not applicable.

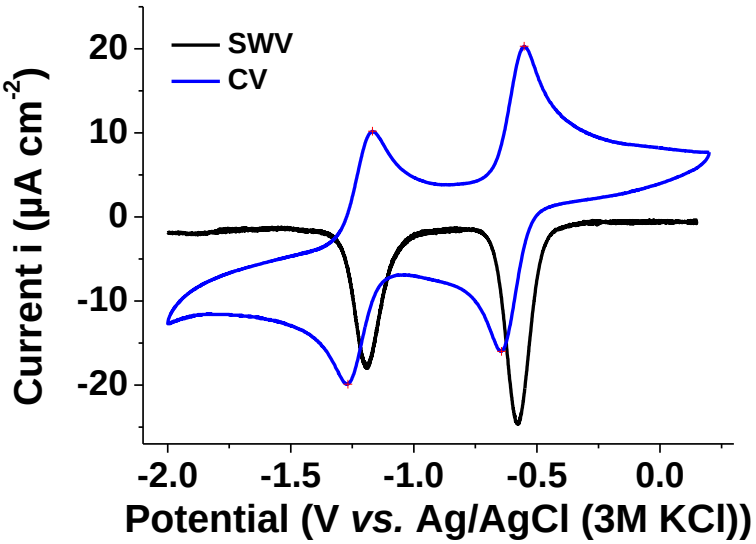

Figure S9. CV (blue curve) and SWV (black curve) spectra of probe **4** (1.63 mM). Solvent: DMSO; *I* = 0.1 M n-Bu_4NPF_6; *v* = 200 mV s^{-1}. Reference electrode = KCl(3M)/Ag/AgCl; working electrode = glassy carbon disk of 0.07 cm^2 area; auxiliary electrode = Pt wire.

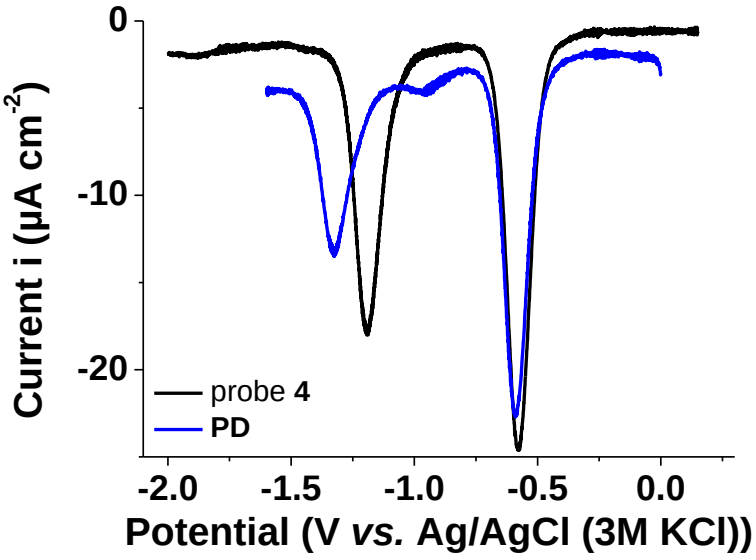

Figure S10. Comparison of the SWV spectra of PD (blue curve) and probe **4** (black curve). Solvent: DMSO; *I* = 0.1 M n-Bu_4NPF_6; *v* = 200 mV s^{-1}. Reference electrode = KCl(3M)/Ag/AgCl; working electrode = glassy carbon disk of 0.07 cm^2 area; auxiliary electrode = Pt wire.

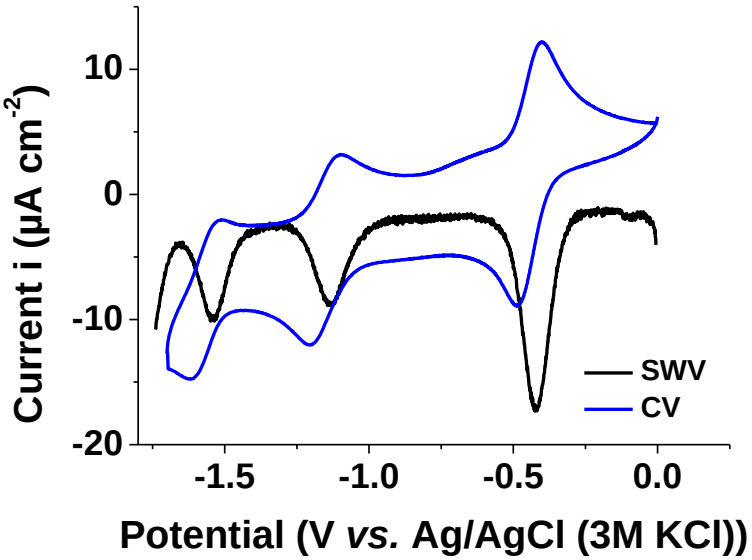

Figure S11. CV (blue curve) and SWV (black curve) spectra of probe **1** (0.97 mM). Solvent: DMSO; *I* = 0.1 M n-Bu_4NPF_6; *v* = 200 mV s^{-1}. Reference electrode = KCl(3M)/Ag/AgCl; working electrode = glassy carbon disk of 0.07 cm^2 area; auxiliary electrode = Pt wire.

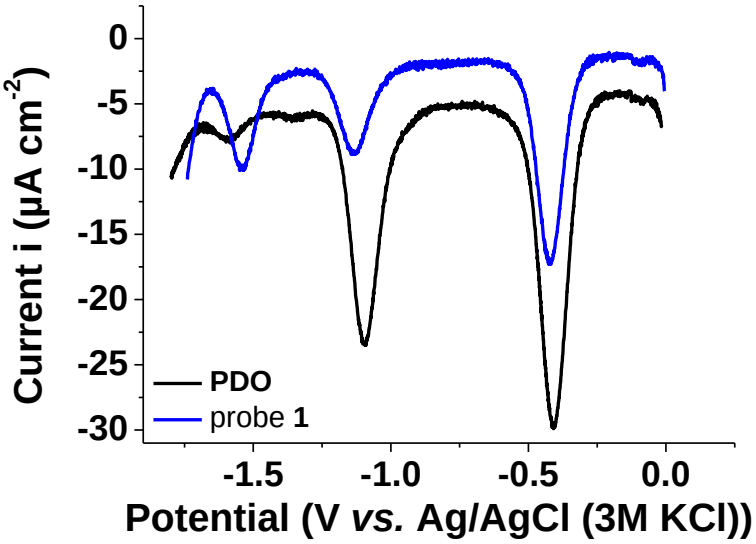

Figure S12. Comparison of the SWV spectra of **PDO** (blue curve) and probe **1** (black curve). Solvent: DMSO; *I* = 0.1 M n-Bu_4NPF_6; *v* = 200 mV s^{-1}. Reference electrode = KCl(3M)/Ag/AgCl; working electrode = glassy carbon disk of 0.07 cm^2 area; auxiliary electrode = Pt wire.

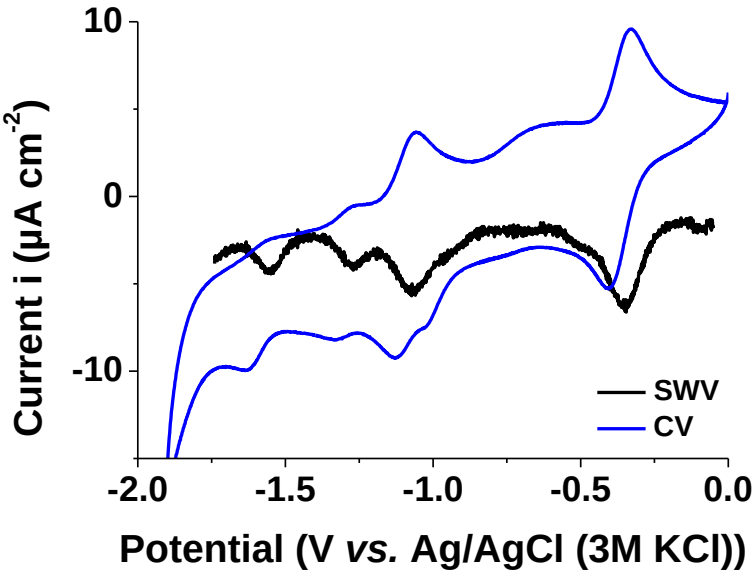

Figure S13. CV (blue curve) and SWV (black curve) spectra of **6-fluoro-PDO** (1.06 mM). Solvent: DMSO; I = 0.1 M n-Bu_4NPF_6; v = 200 mV s^{-1}. Reference electrode = KCl(3M)/Ag/AgCl; working electrode = glassy carbon disk of 0.07 cm^2 area; auxiliary electrode = Pt wire.

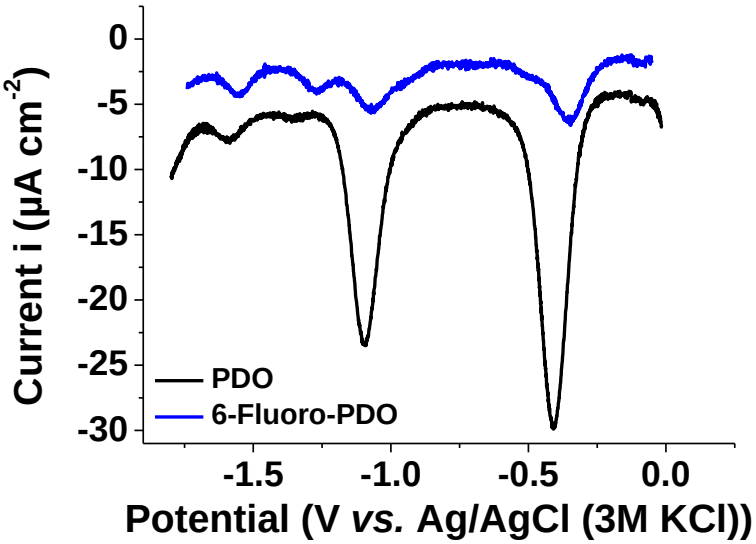

Figure S14. Comparison of the SWV spectra of **6-fluoro-PDO** (blue curve) and **PDO** (black curve). Solvent: DMSO; I = 0.1 M n-Bu_4NPF_6; v = 200 mV s^{-1}. Reference electrode = KCl(3M)/Ag/AgCl; working electrode = glassy carbon disk of 0.07 cm^2 area; auxiliary electrode = Pt wire.

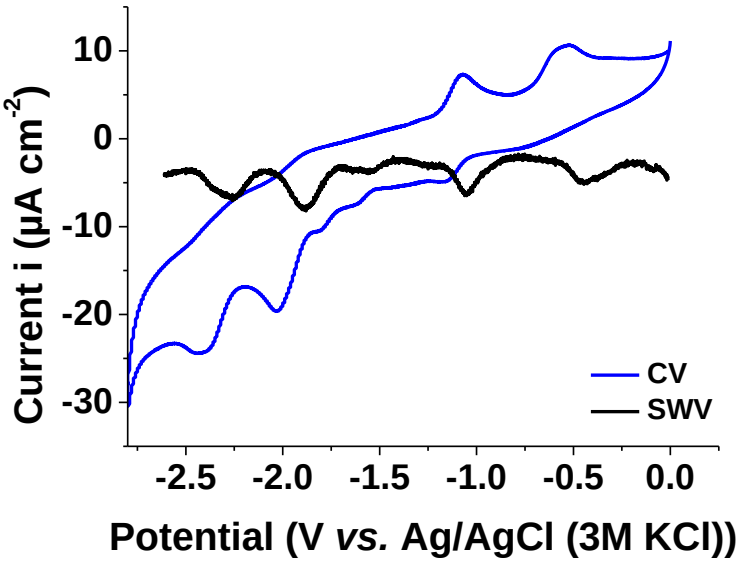

Figure S15. CV (blue curve) and SWV (black curve) spectra of probe **3** (1 mM). Solvent: DMSO; *I* = 0.1 M n-Bu_4NPF_6; *v* = 200 mV s^{-1}. Reference electrode = KCl(3M)/Ag/AgCl; working electrode = glassy carbon disk of 0.07 cm^2 area; auxiliary electrode = Pt wire.

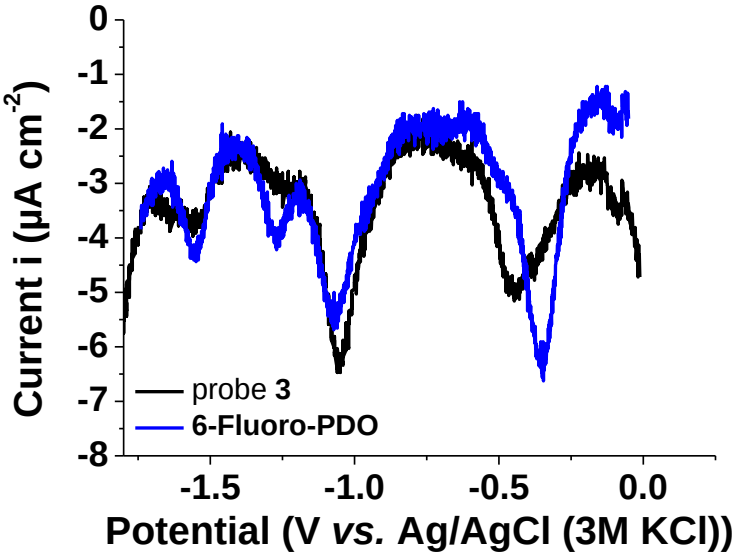

Figure S16. Comparison of the SWV spectra of **6-fluoro-PDO** (blue curve) and probe **3** (black curve). Solvent: DMSO; *I* = 0.1 M n-Bu_4NPF_6; *v* = 200 mV s^{-1}. Reference electrode = KCl(3M)/Ag/AgCl; working electrode = glassy carbon disk of 0.07 cm^2 area; auxiliary electrode = Pt wire.

B2.5. Optimization of the peptide GSH photolabeling in the presence of new probe 3

To characterize the photoreactive properties of probe **3,** different conditions were tested to optimize this step using the glutathione tripeptide (GSH) as a protein surrogate, by changing GSH and probe concentrations, buffer composition and duration of UV irradiation. All the reactions of photolabeling were performed in deoxygenated conditions with irradiation at 350 nm using a Rayonet photochemical reactor equipped with eight RPR-3500A lamps of 200 W. First, the photolabeling properties of probe **3** were tested in comparison to other probes previously synthesized. [19] Using the same conditions as Cichocki and co-workers,[19] incubation of GSH and probe **3** was performed in 50% ACN conditions, with a final concentration of the probe of 600 µM and 8-fold molar excess of GSH. The irradiation was performed over different durations, from 5 to 420 minutes, and we measured the quantity of specific GSH-probe **3** adduct generated during the reaction, as well as that of unreacted probe **3** by LC-MS (Figure S9). On the extracted ion chromatograms (EIC), the retention time of the GSH-probe **3** adduct (*m/z* 626.14), and of the non-reacted probe **3** (*m/z* 319.09) were 28.8 min and 39.3 min, respectively. Photolabeling yields, calculated as the area of the GSH-probe **3** adduct divided by the total of the two areas of probe **3** (reacted and unreacted), were better at shorter photoirradiation times, with 8, 9 and 13% for the 5, 10 and 15 minutes of irradiation, respectively.

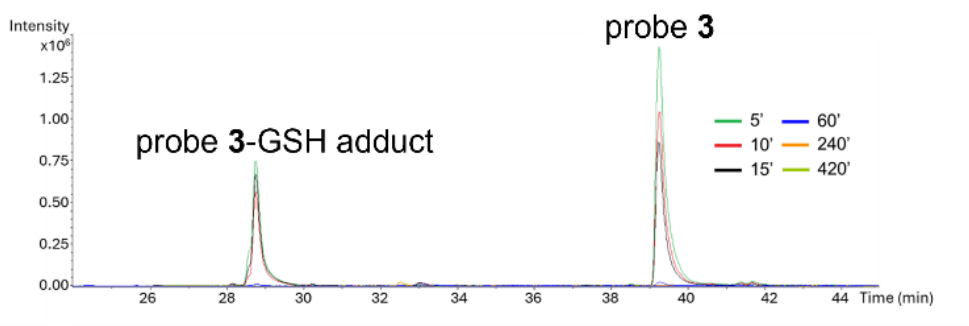

Figure S17. Extracted ion chromatograms relative to the non-labelled probe **3** and probe **3**-GSH adduct relative to the photo-reaction of the two species for 5, 10, and 15 minutes, in green, red and, black respectively.

The photolabeling yield was then investigated in the ABPP conditions procedure, by using a buffer containing a final percentage of 10% ACN and a final concentration of 10 µM probe **3**. In these operative conditions, no probe-peptide adduct was observed (data not shown). Finally, the yield of GSH photolabeling was optimized to 21%, upon 15 minutes of irradiation, by adding 10% propan-2-ol and a final probe concentration of 10 µM to the reaction mixture (Figure S10). According to the optimized condition #5, the click reaction was carried out with the probe **3**. Figure S10 reports the EIC chromatograms of probe **3** with a retention time of about 39.3 min (*m/z* 319.09) and of biotinylated probe **3** with a retention time of about 31.3 min (*m/z* 719.27). Peak +16 may account for the formation of the Probe **3**-GSH adduct with oxygen atom insertion at the sulfur atom of GSH. The results on the click reaction with probe **3** were comparable to those obtained with probe **1**.

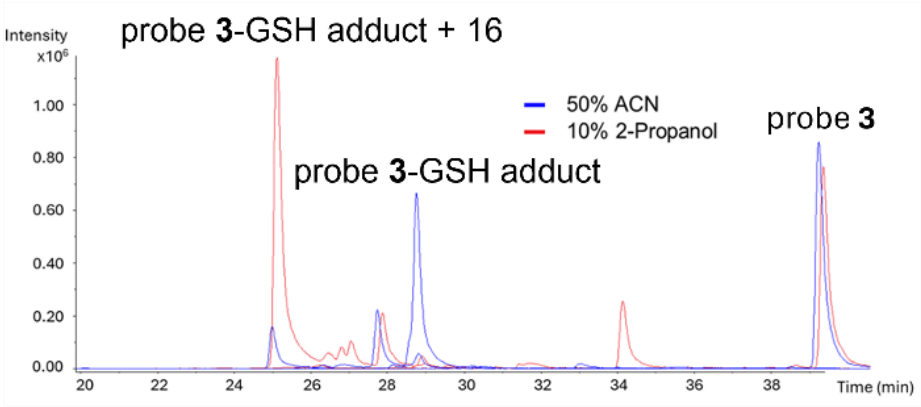

Figure S18. Extracted ion chromatograms (EIC) of the reaction between probe **3** and the tripeptide GSH in the presence of 10% propan-2-ol and upon 15 min of UV photoirradiation.

B2.6. Proteome analysis of *S. cerevisiae* strains by MS analysis

Protein lysates from wild-type (WT) and *ΔNDE1* were subjected to a shotgun proteomics approach using SP3 mediated digestion, and analyzed by nanoLC-MS/MS on a Q-Ex+ mass spectrometer. The raw data were analyzed by MaxQuant for protein identification and quantification.[49] Statistical analysis were performed with the software Perseus.[50] 1710 proteins were identified with at least 3 peptides and 1% false discovery rate (FDR) by Maxquant searching in the Swissprot *S. cerevisiae* database. Of these, 1556 proteins passed Perseus software filtering (i.e., reverse proteins, contaminants, and proteins with 50% of valid values in at least one group), which represents 26% of the approx. 6000 orfs contained in the yeast genome. The missing LFQ intensity values were imputed from the normal distribution of the data. We detected 224 differentially expressed proteins between *ΔNDE1* and WT samples (Student's t-test using a 5% FDR – Benjamini-Hochberg adjusted p-value), 20 up- and 30 down-regulated by more than 2 folds in the mutant compared to WT (Figure S11 and Supplementary Table S1). As expected, the most down-regulated protein in the mutant is Nde1. In fact, no peptides belonging to this protein was identified in the deleted strain *ΔNDE1*.

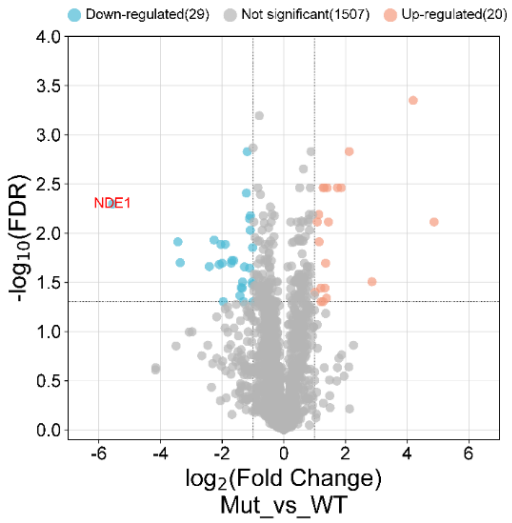

Figure S19. Volcano plot of the differentially expressed proteins in yeast WT and *ΔNDE1* samples. Proteins that are down- and up- regulated by at least 2-fold in *ΔNDE1* compared to WT, are highlighted in blue and red, respectively.

C. Data Deposition

The mass spectrometry proteomics data have been deposited to the ProteomeXchange Consortium via the PRIDE[51] partner repository with the dataset identifier PXD050982 and Project DOI: 10.6019/PXD050982

D. NMR spectra

^{1}H NMR (400 MHz, $CDCl_3$) – 1

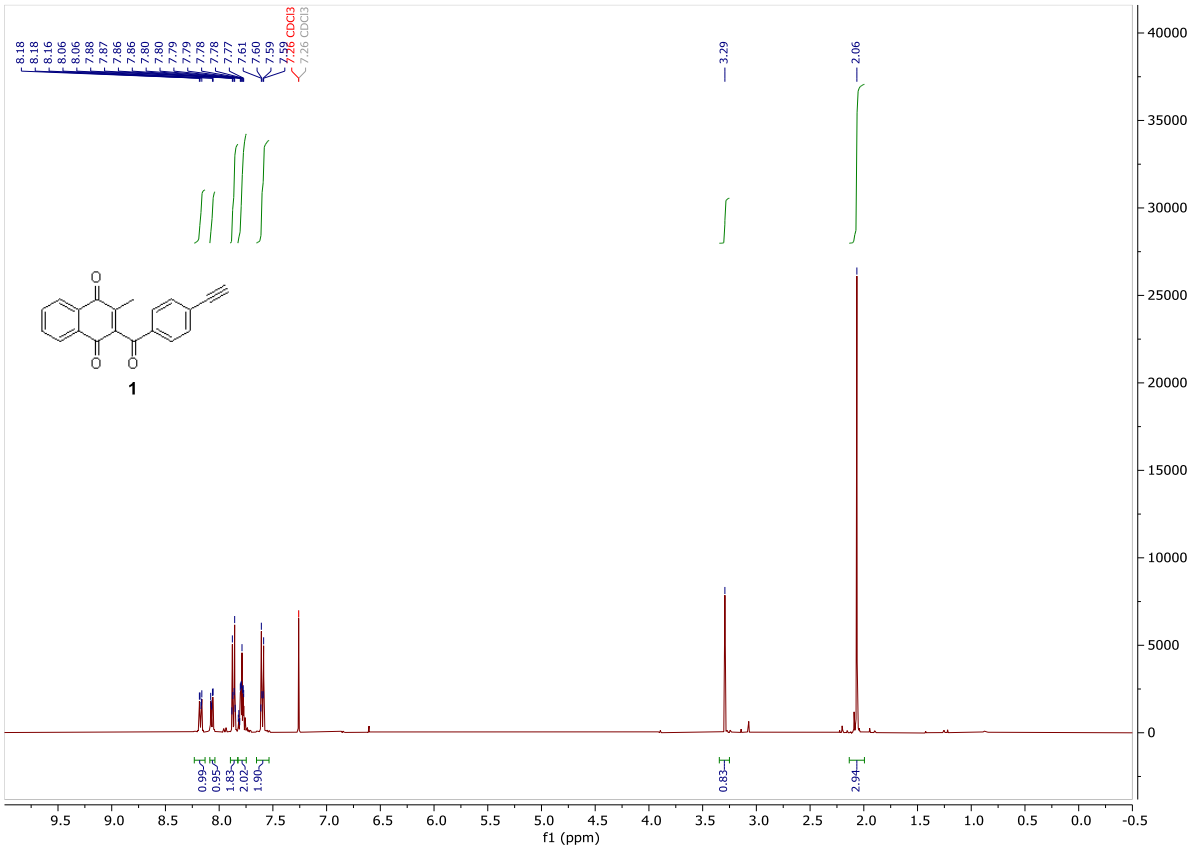

^{1}H NMR (400 MHz, $CDCl_3$) – 3

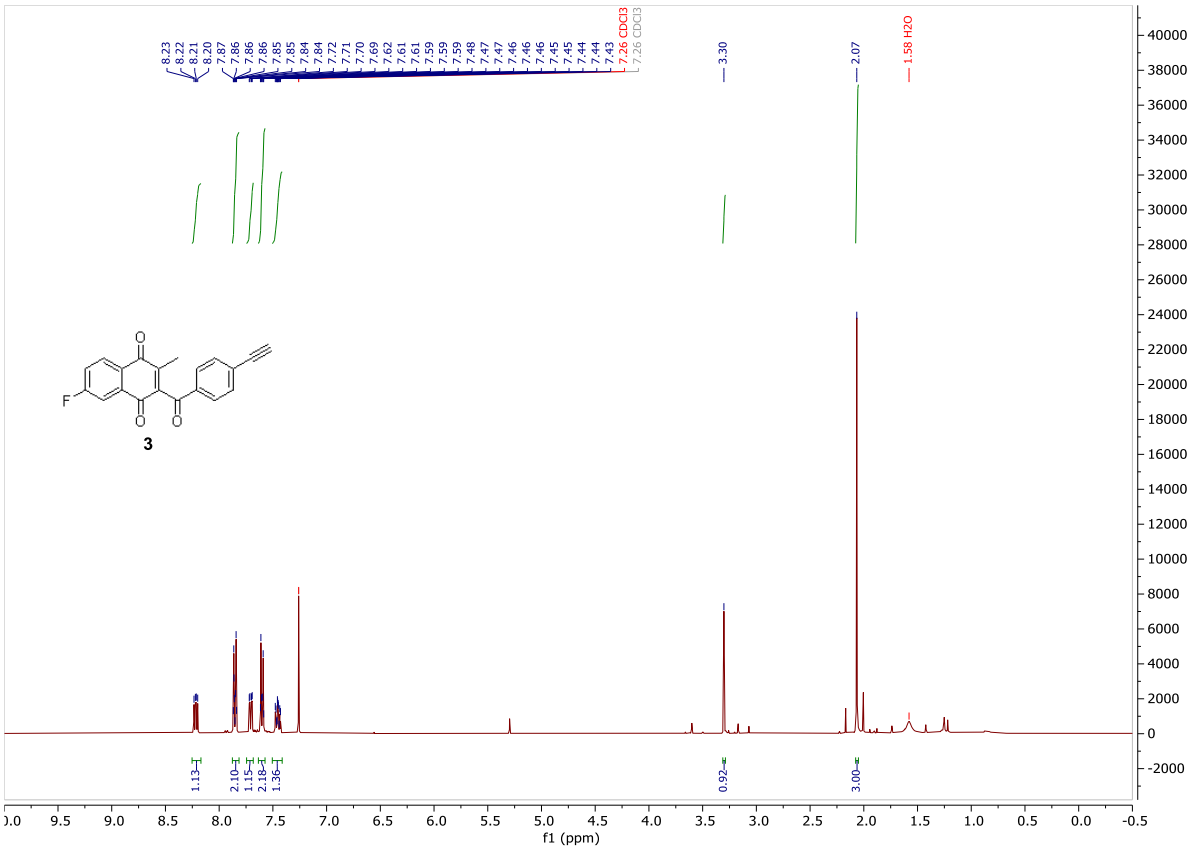

^{19}F {^{1}H} NMR (377 MHz, $CDCl_3$) – 3

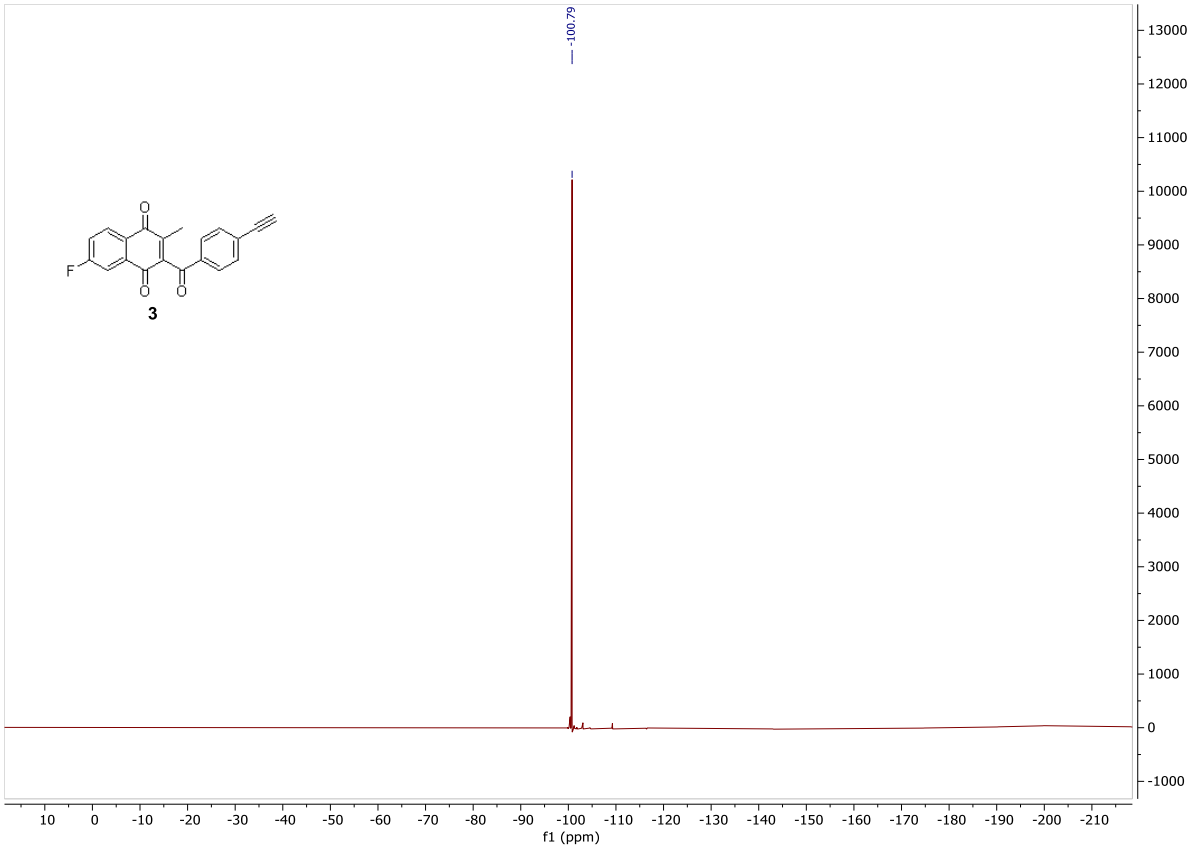

^{13}C {^{1}H} NMR (126 MHz, $CDCl_3$) – 3

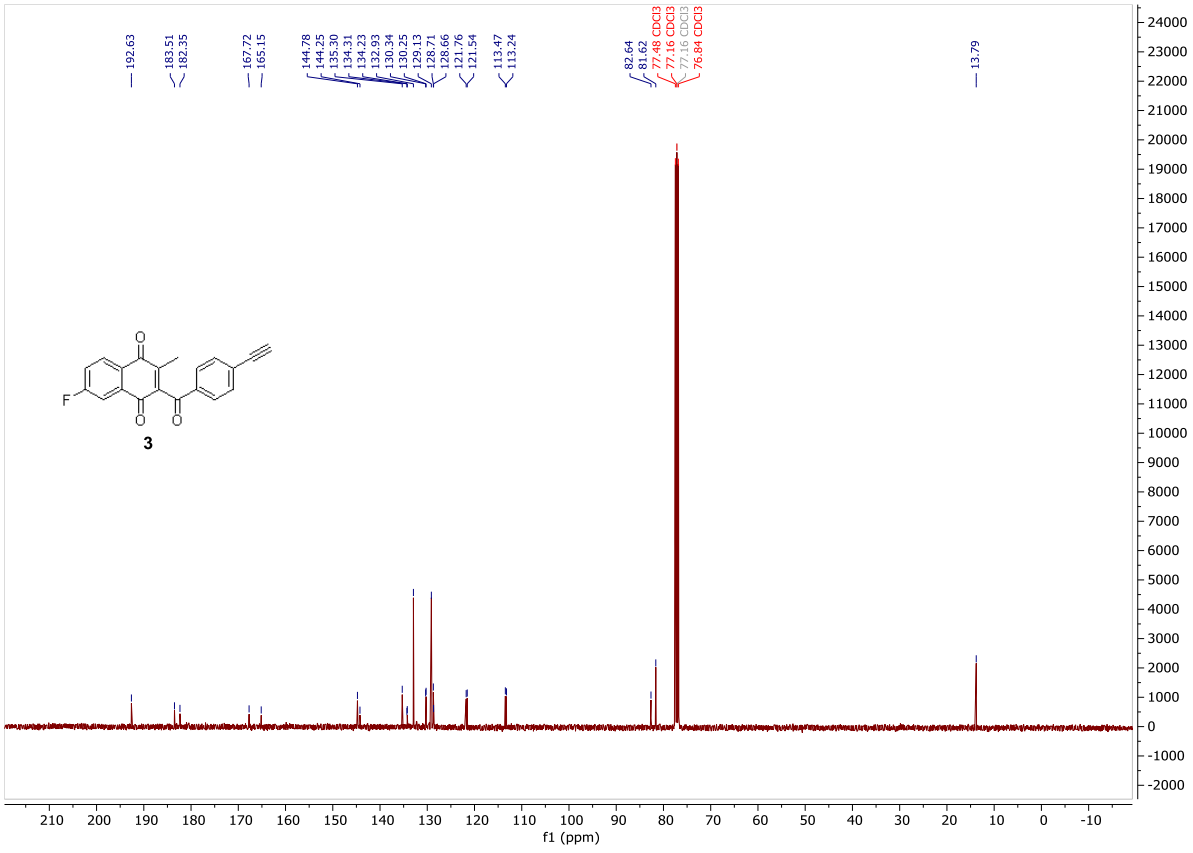

^{1}H NMR (400 MHz, $CDCl_3$) – 4

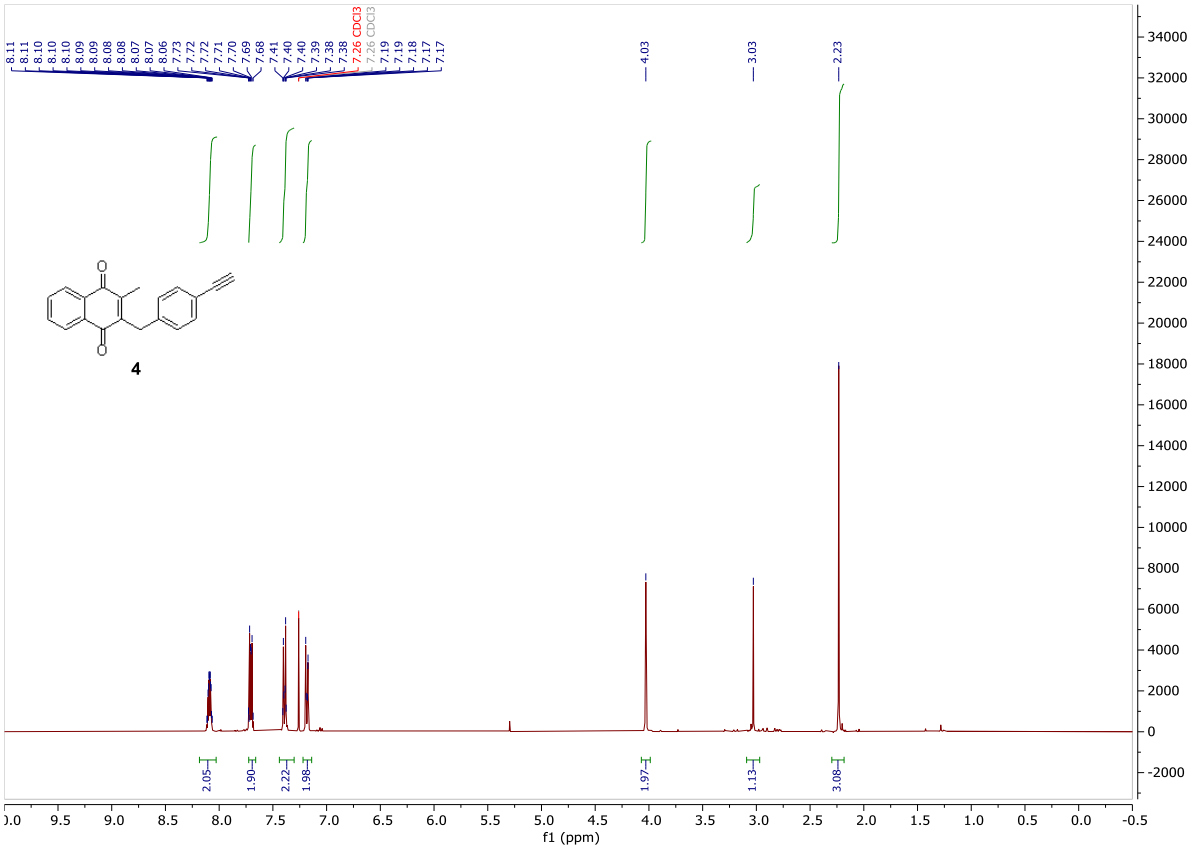

^{1}H NMR (400 MHz, $CDCl_3$) – 5

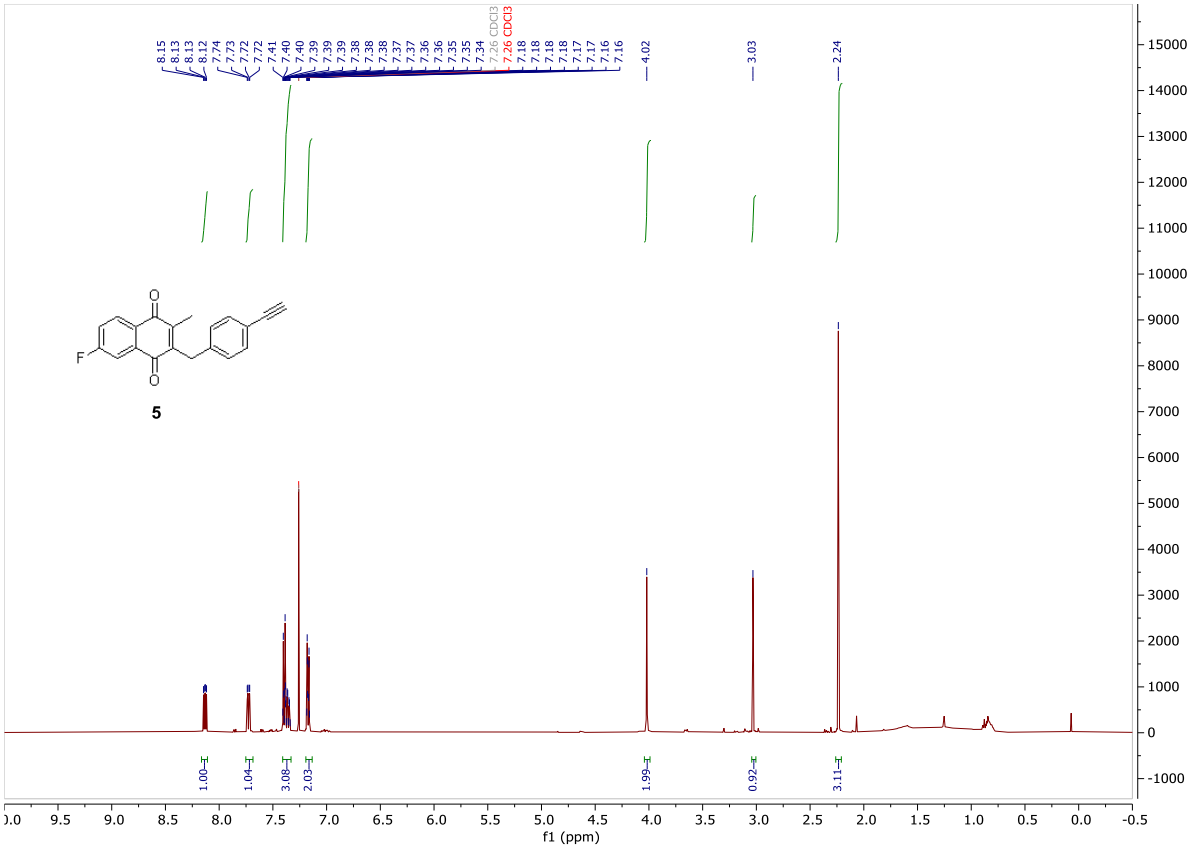

^{19}F {^{1}H} NMR (377 MHz, $CDCl_3$) – 5

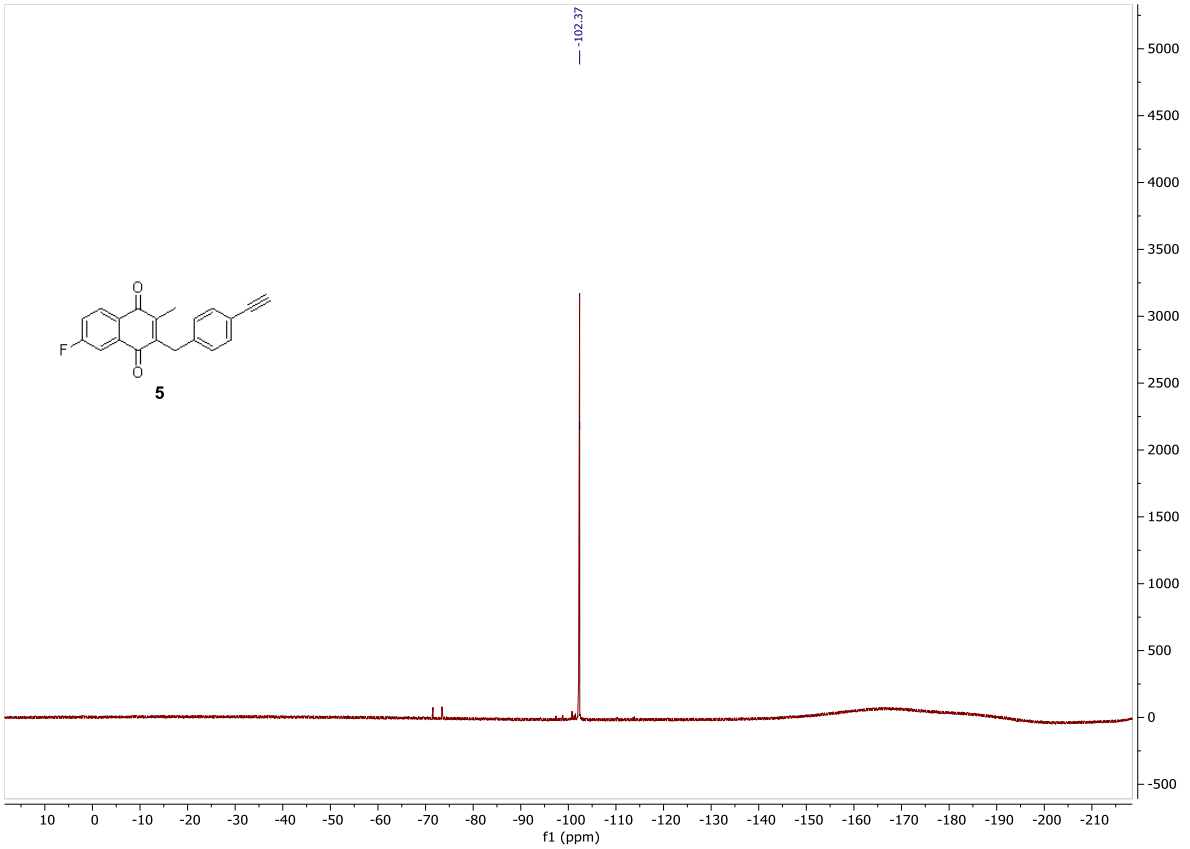

^{13}C {^{1}H} NMR (126 MHz, $CDCl_3$) – 5

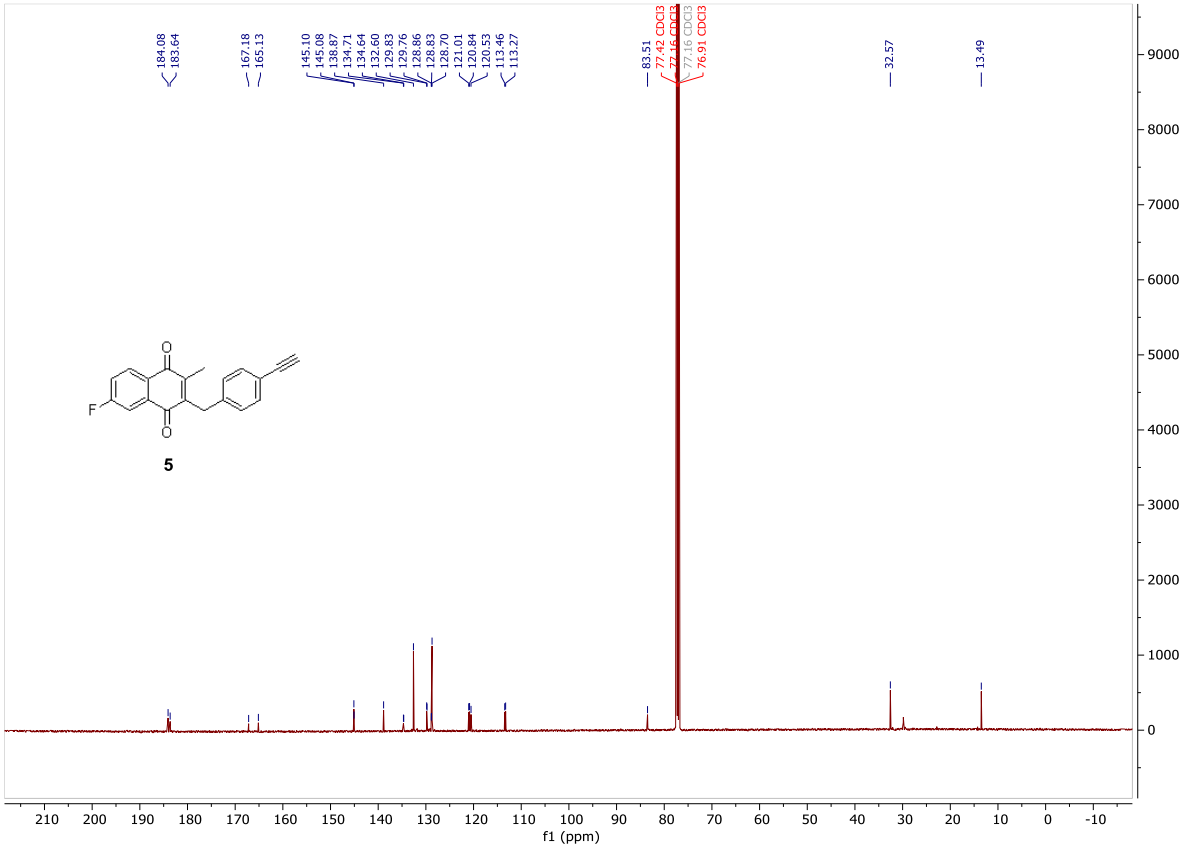

^{1}H NMR (400 MHz, $CDCl_3$) – 11

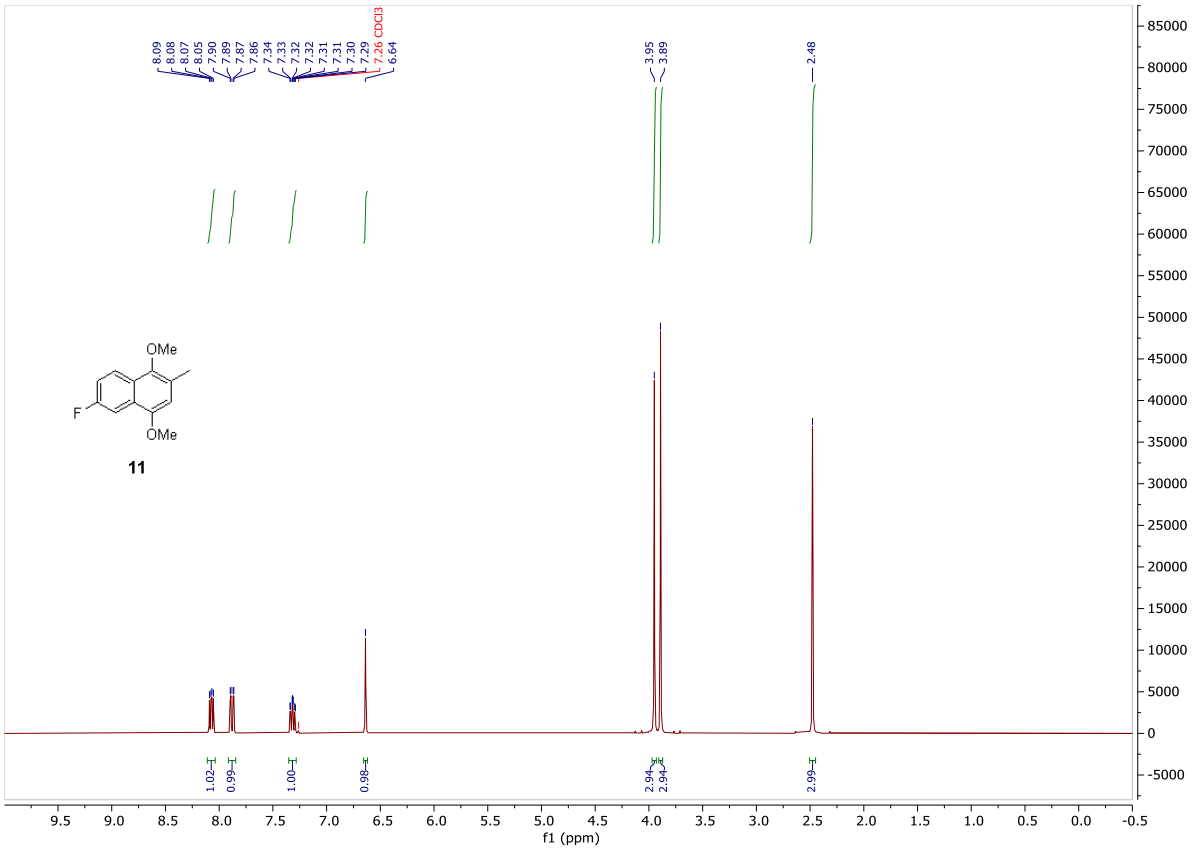

^{19}F {^{1}H} NMR (377 MHz, $CDCl_3$) – 11

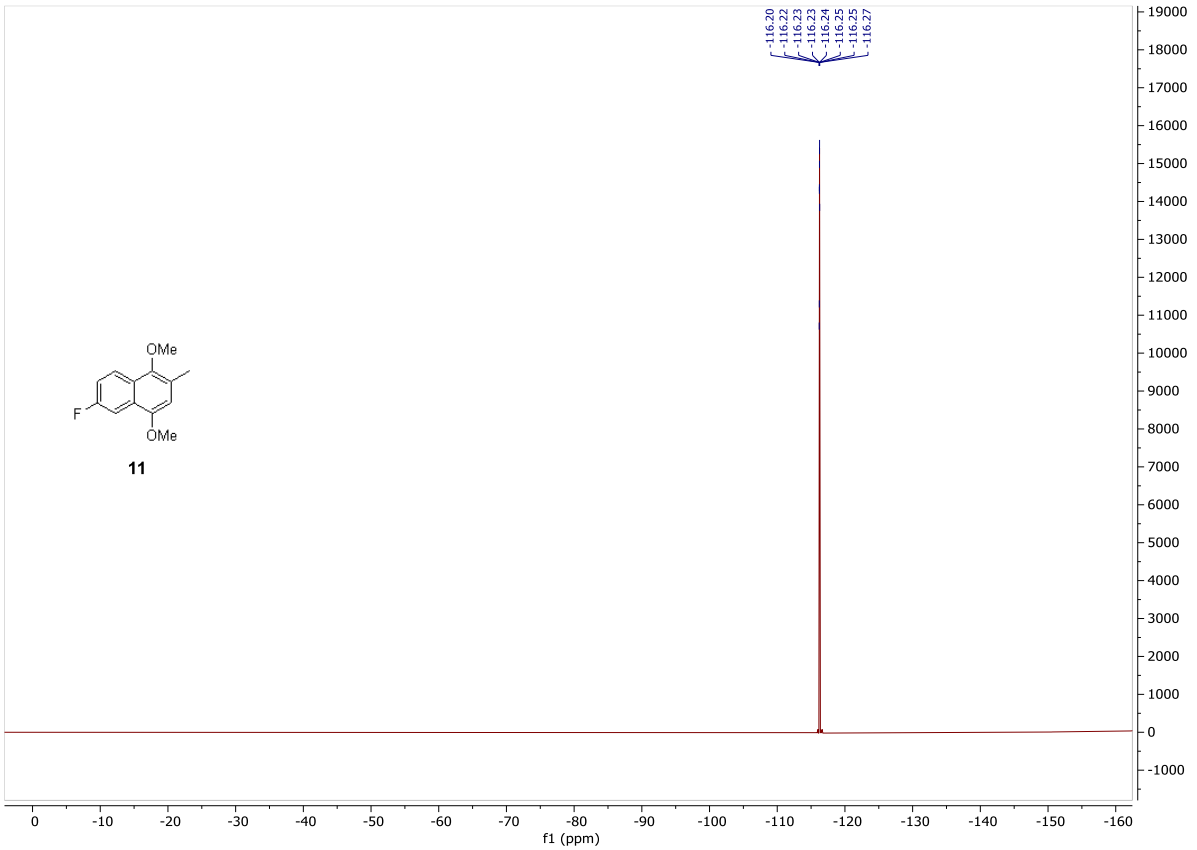

^{13}C {^{1}H} NMR (126 MHz, $CDCl_3$) – 11

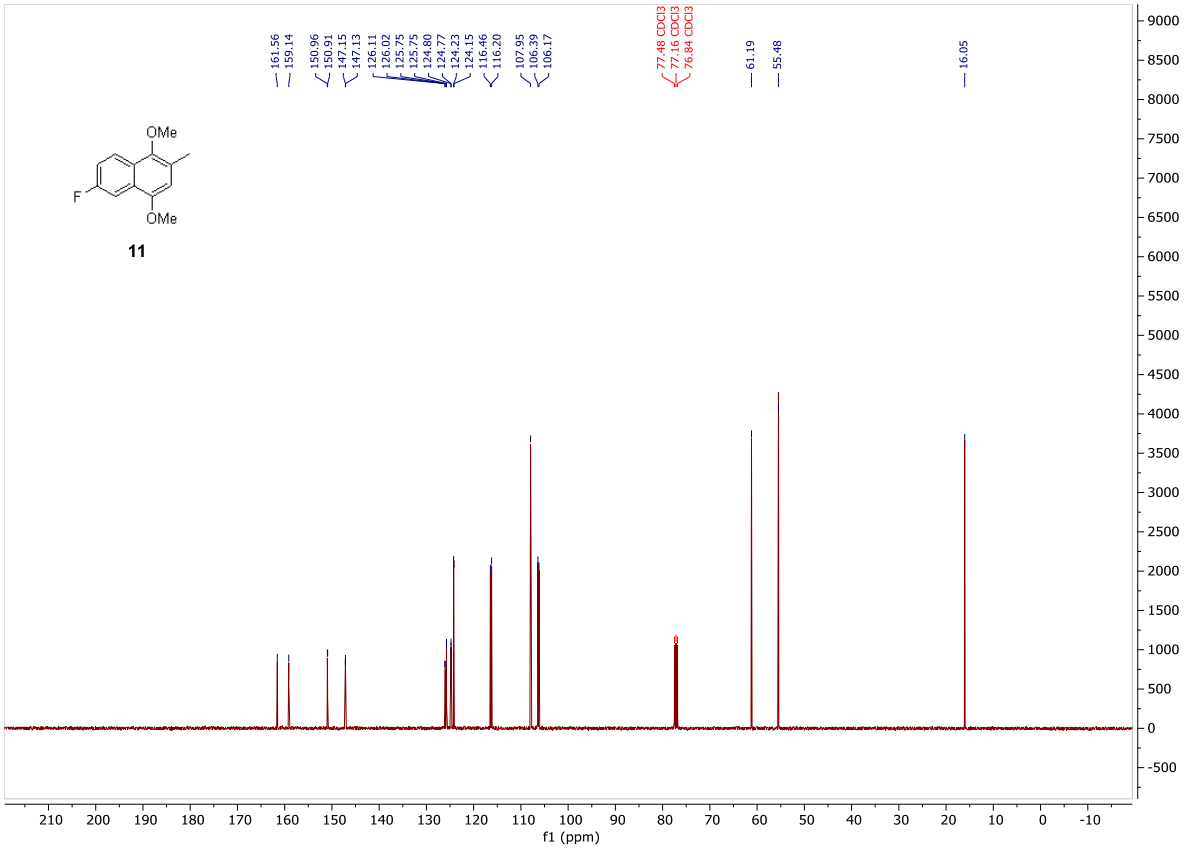

^{1}H NMR (400 MHz, $CDCl_3$) – 12

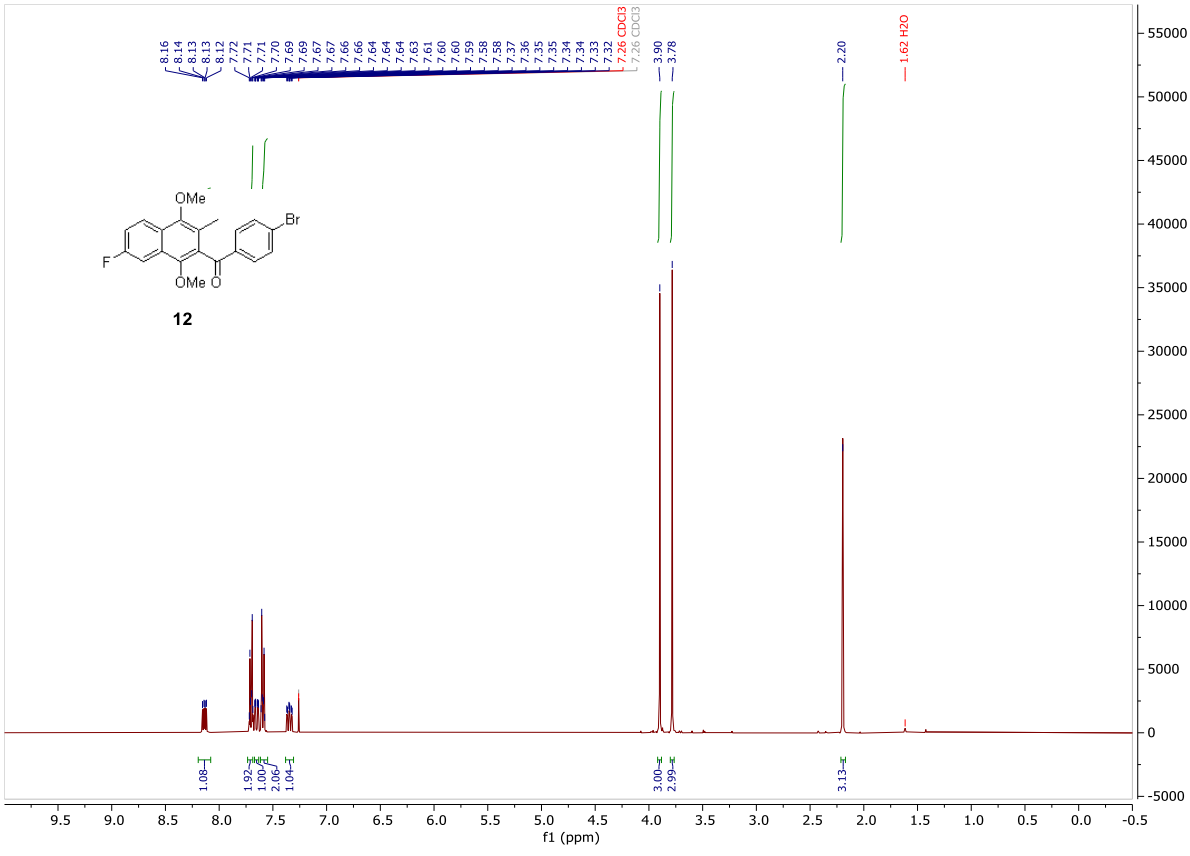

^{19}F {^{1}H} NMR (377 MHz, $CDCl_3$) – 12

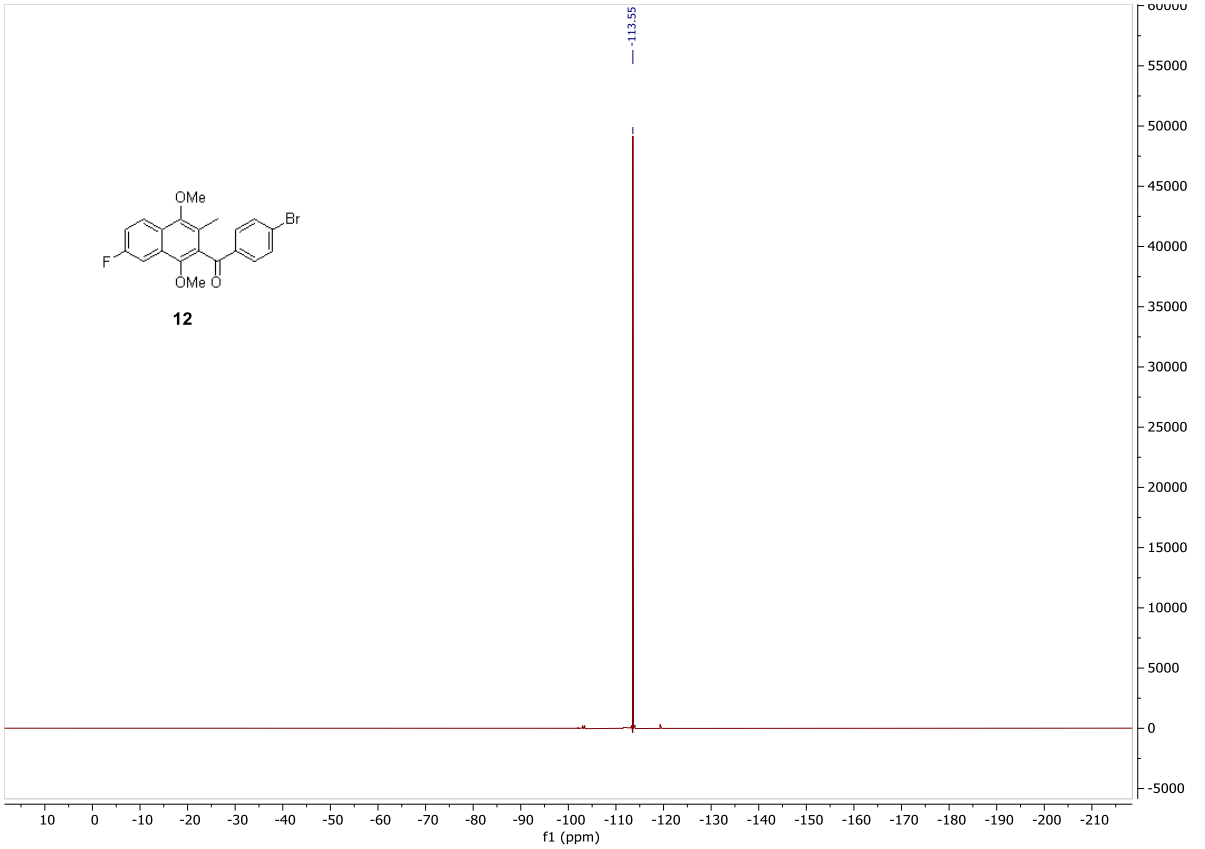

^{13}C {^{1}H} NMR (126 MHz, $CDCl_3$) – 12

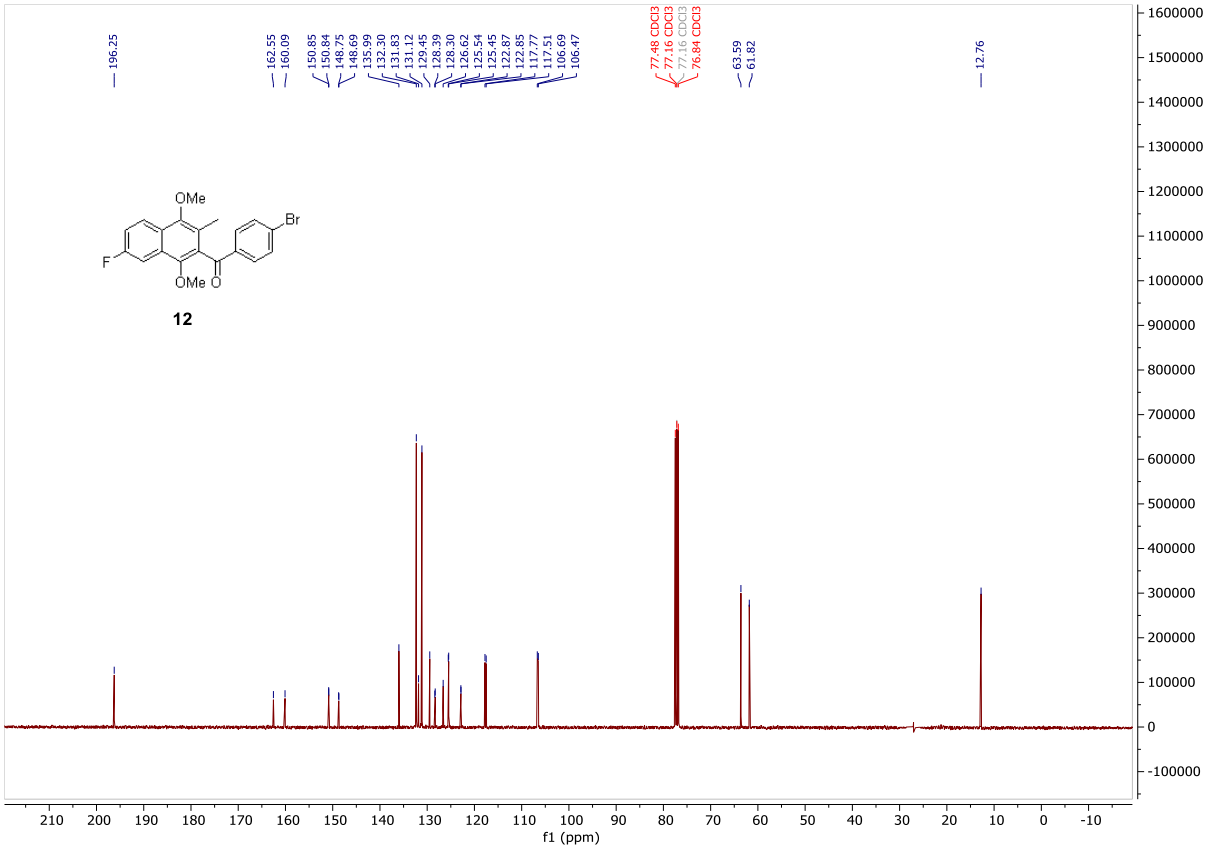

^{1}H NMR (400 MHz, $CDCl_3$) – 13

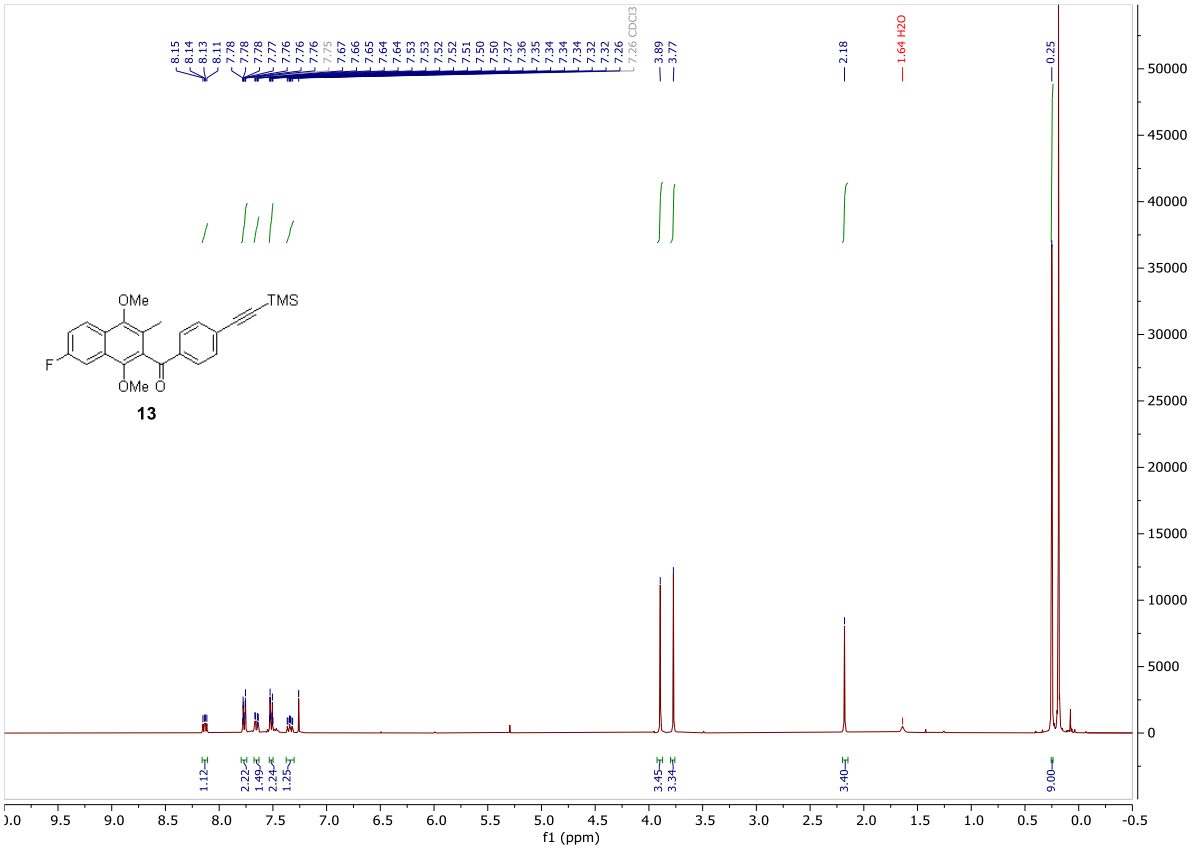

^{19}F {^{1}H} NMR (377 MHz, $CDCl_3$) – 13

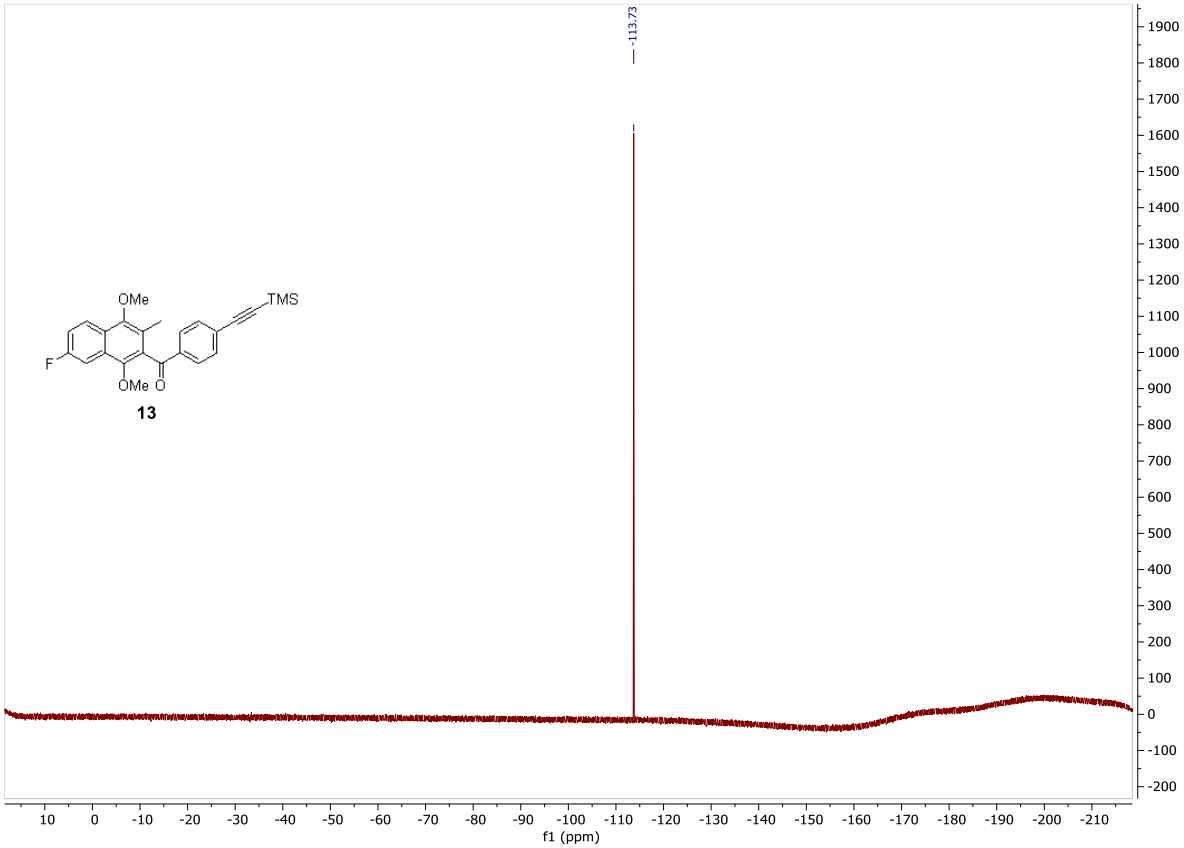

^{13}C {^{1}H} NMR (126 MHz, $CDCl_3$) – 13

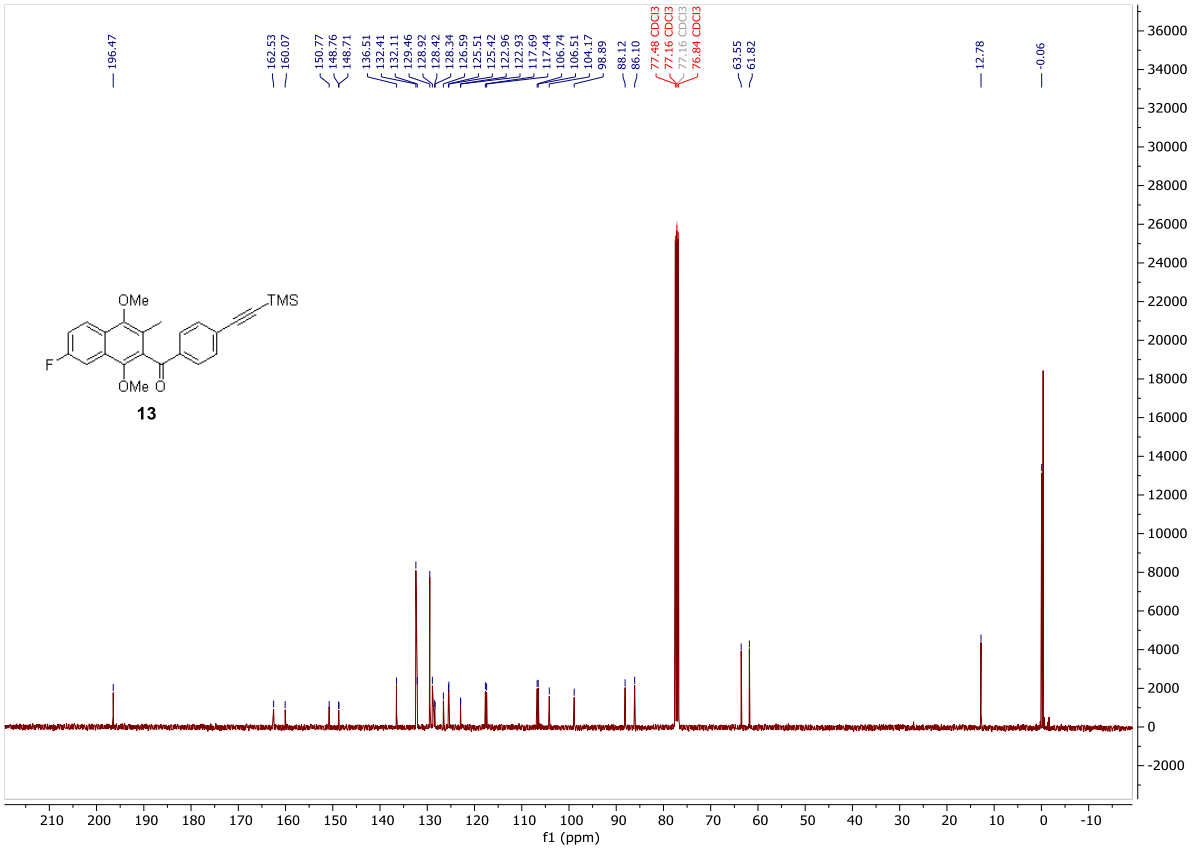

^{1}H NMR (400 MHz, $CDCl_3$) – 14

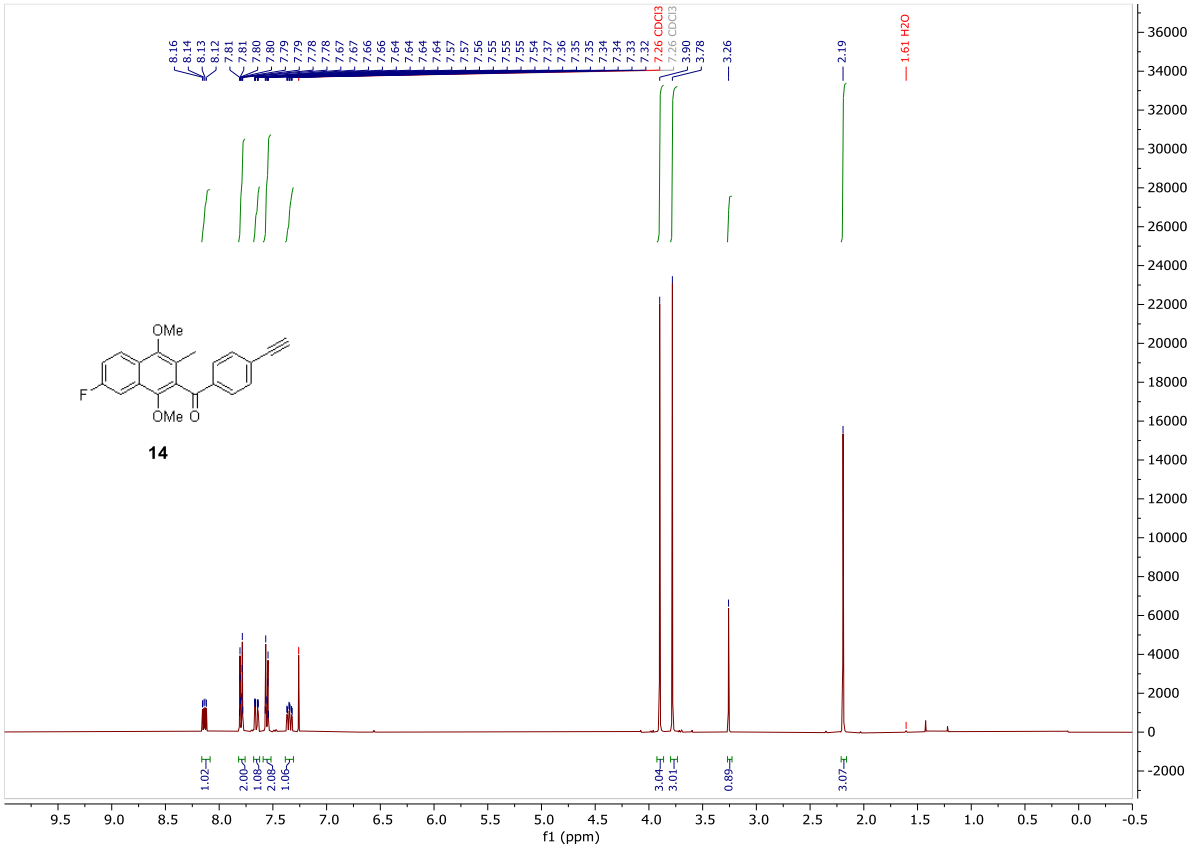

^{19}F {^{1}H} NMR (377 MHz, $CDCl_3$) – 14

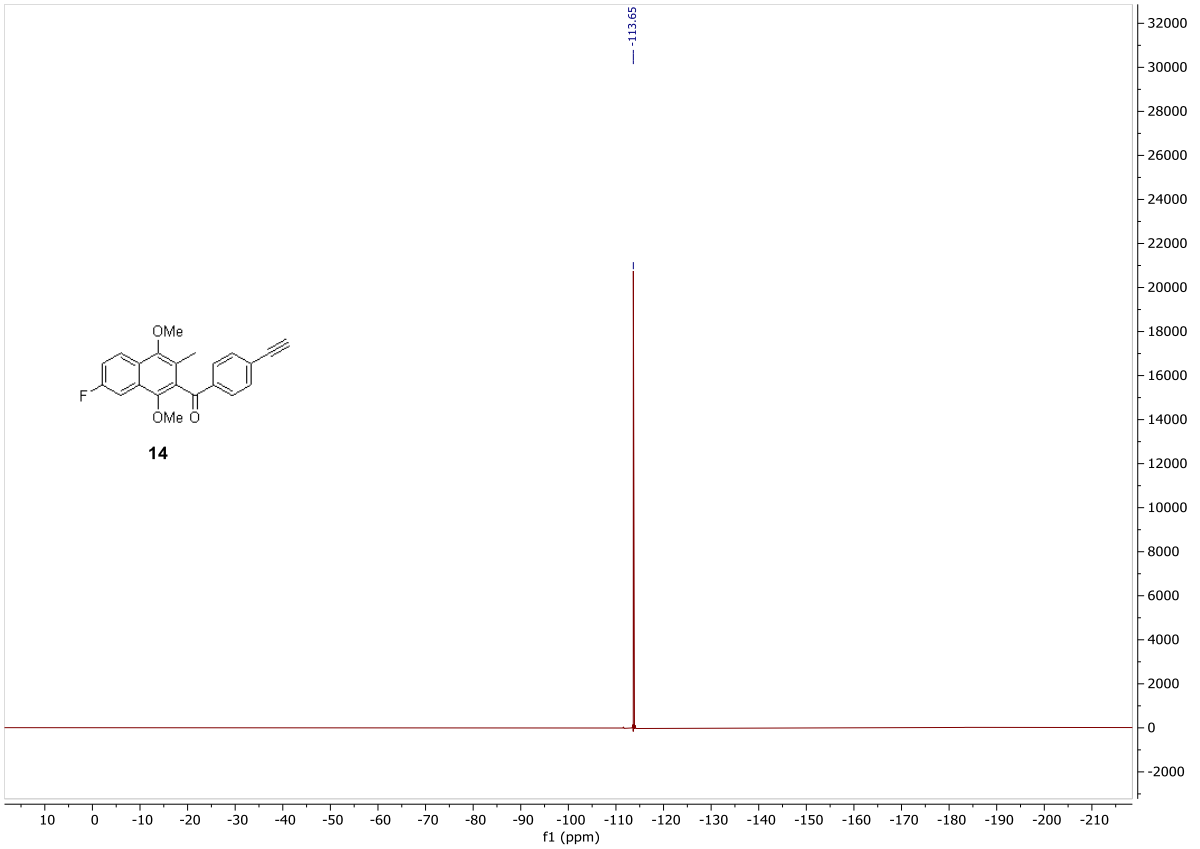

^{13}C {^{1}H} NMR (126 MHz, $CDCl_3$) – 14

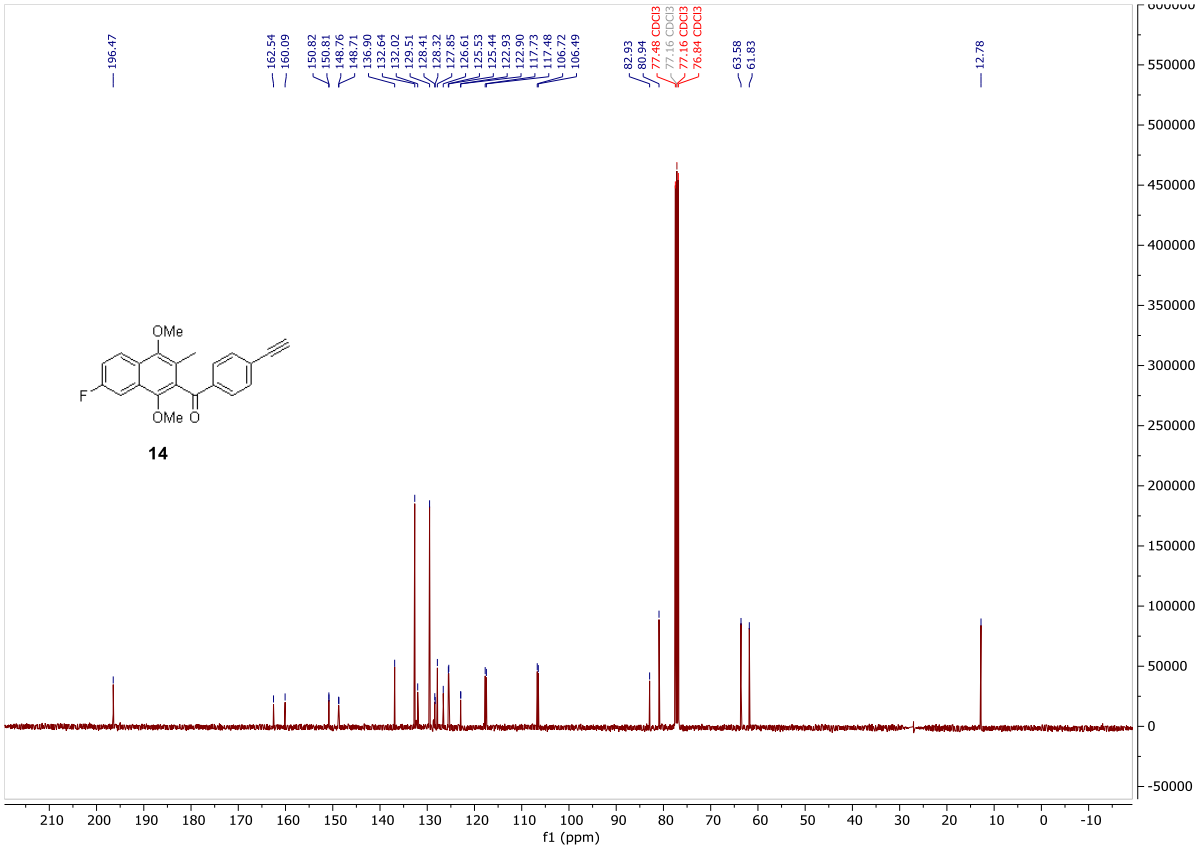

^{1}H NMR (400 MHz, $CDCl_3$) – 19

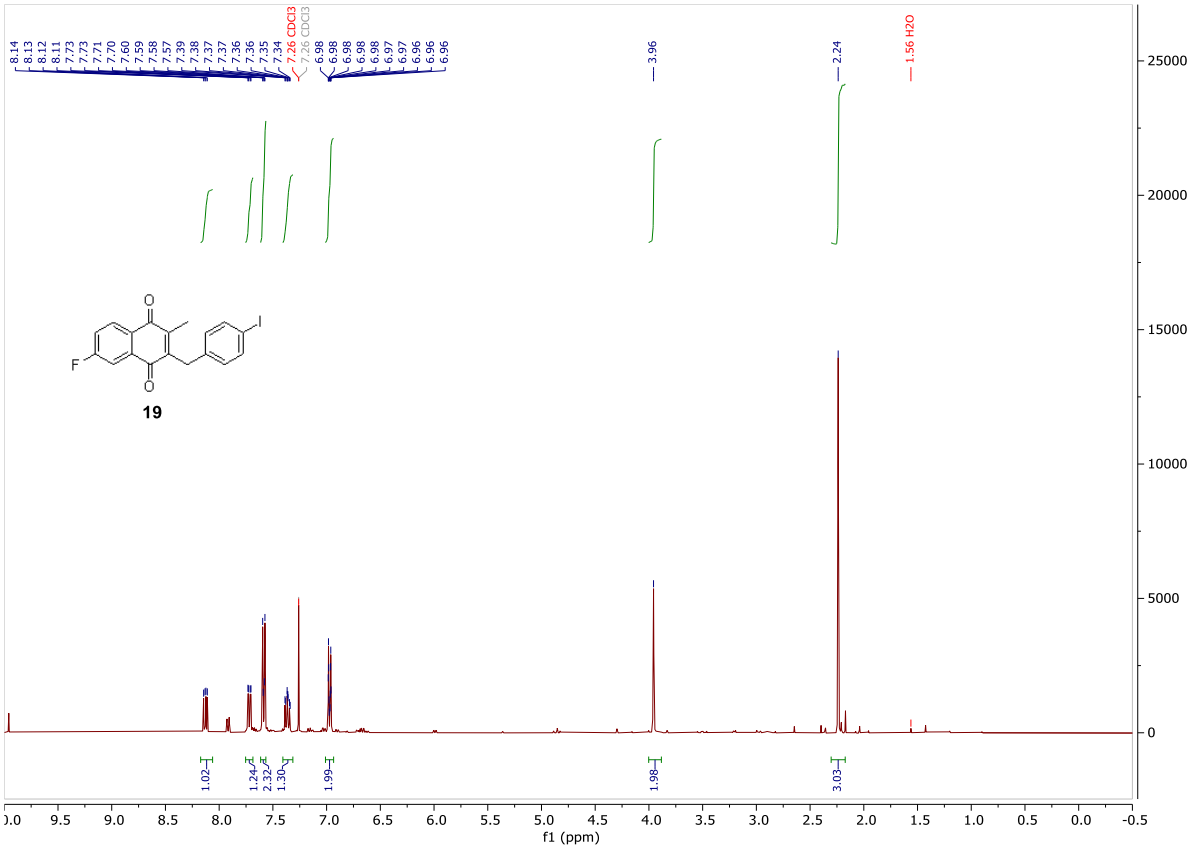

19

^{19}F {^{1}H} NMR (377 MHz, $CDCl_3$) – 19

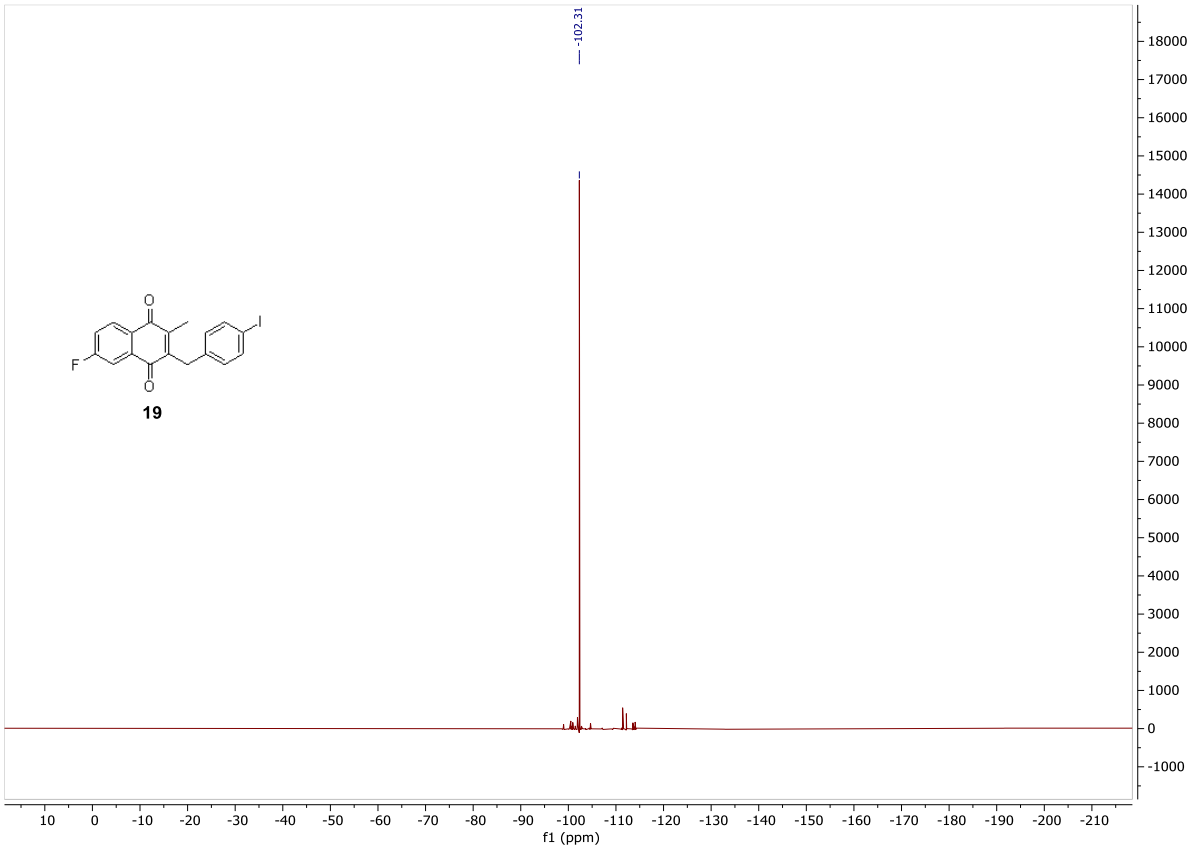

19

^{13}C {^{1}H} NMR (126 MHz, $CDCl_3$) – 19

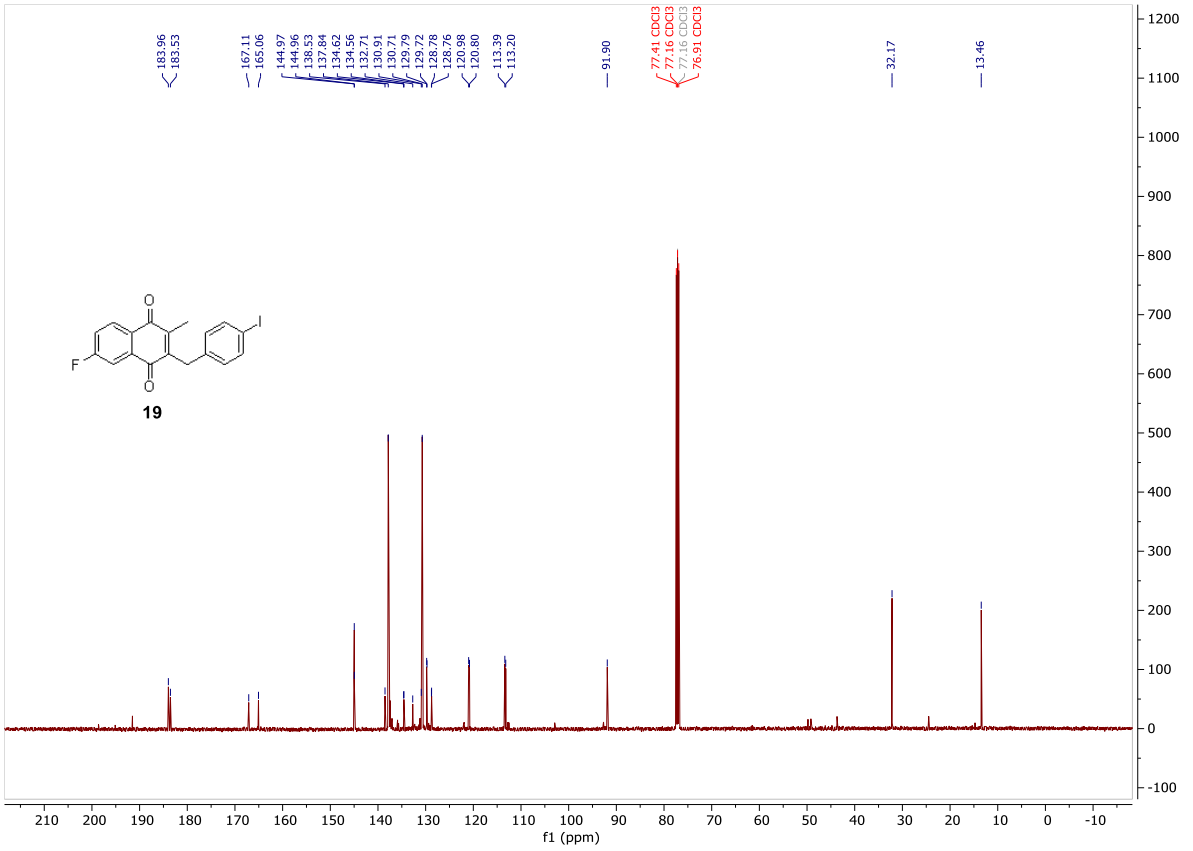

^{1}H NMR (400 MHz, $CDCl_3$) – 20

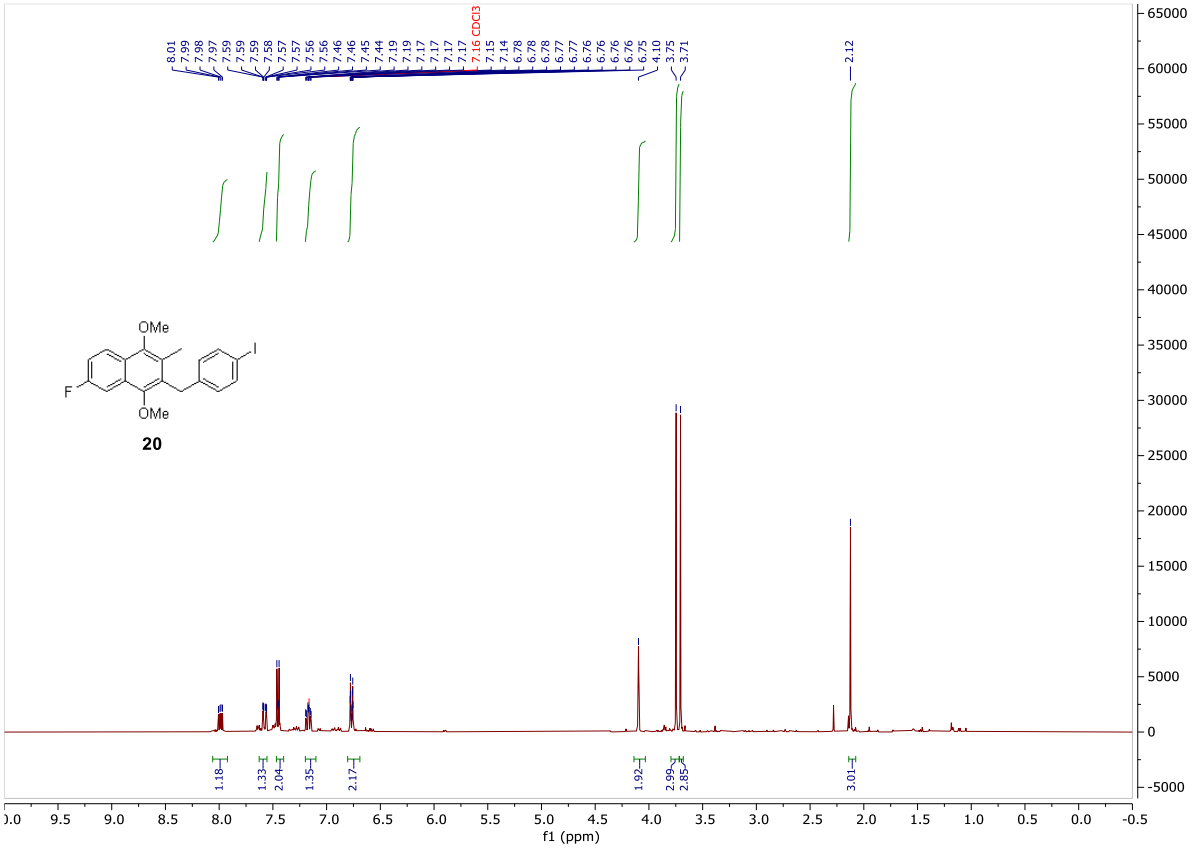

^{19}F {^{1}H} NMR (377 MHz, $CDCl_3$) – 20

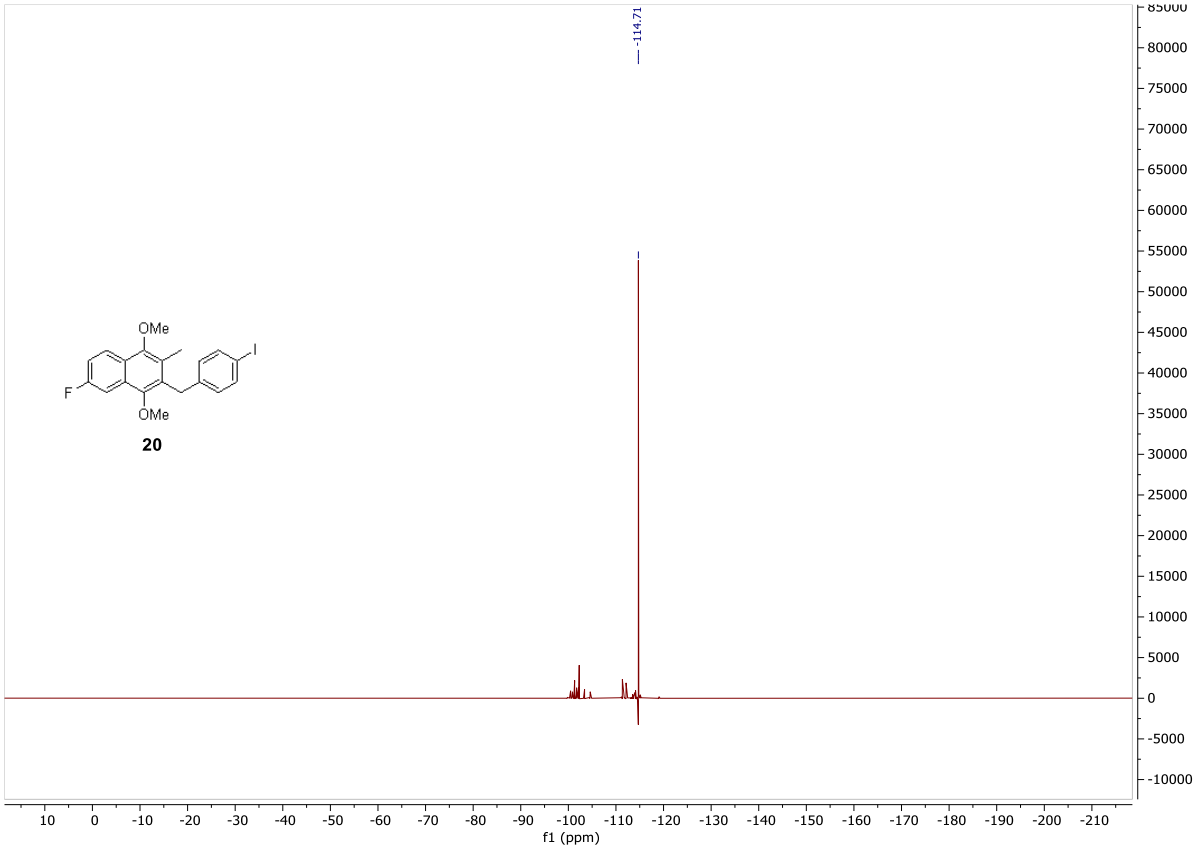

^{13}C {^{1}H} NMR (101 MHz, $CDCl_3$) – 20

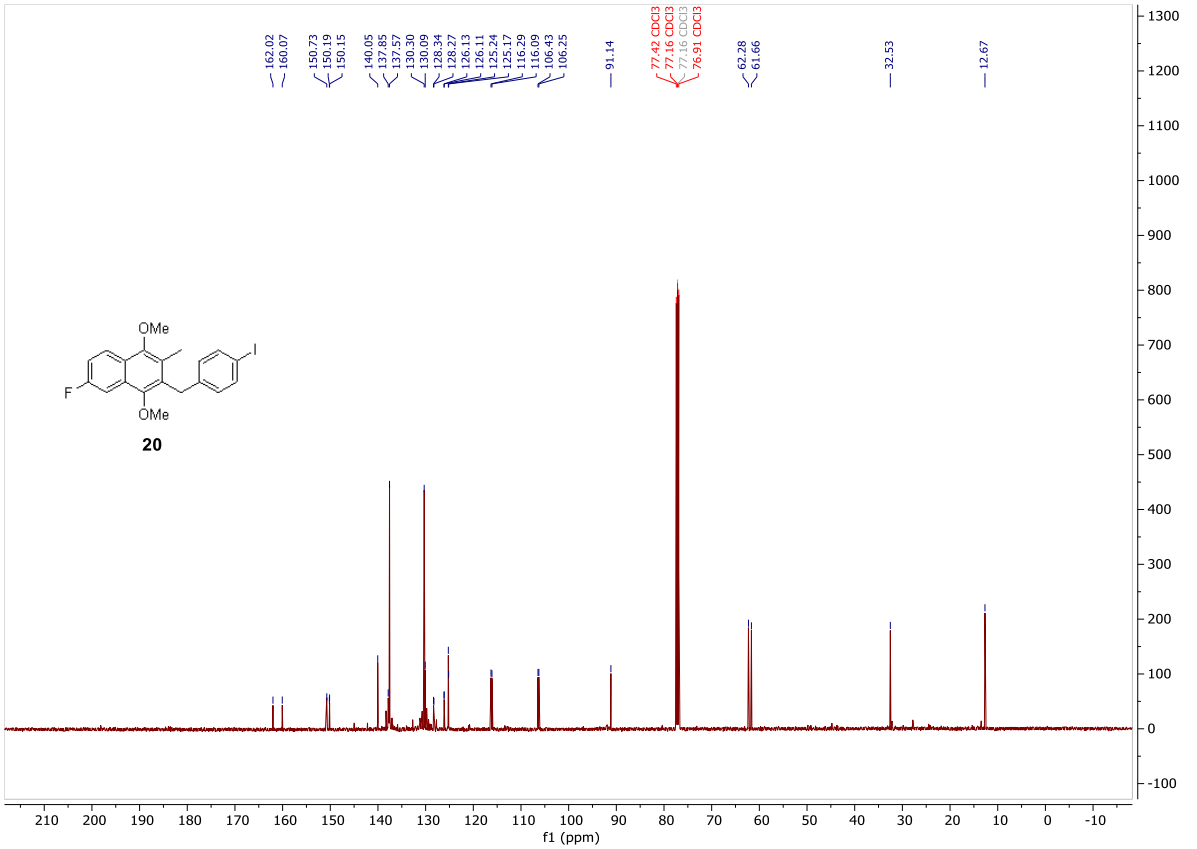

^{1}H NMR (400 MHz, $CDCl_3$) – 21

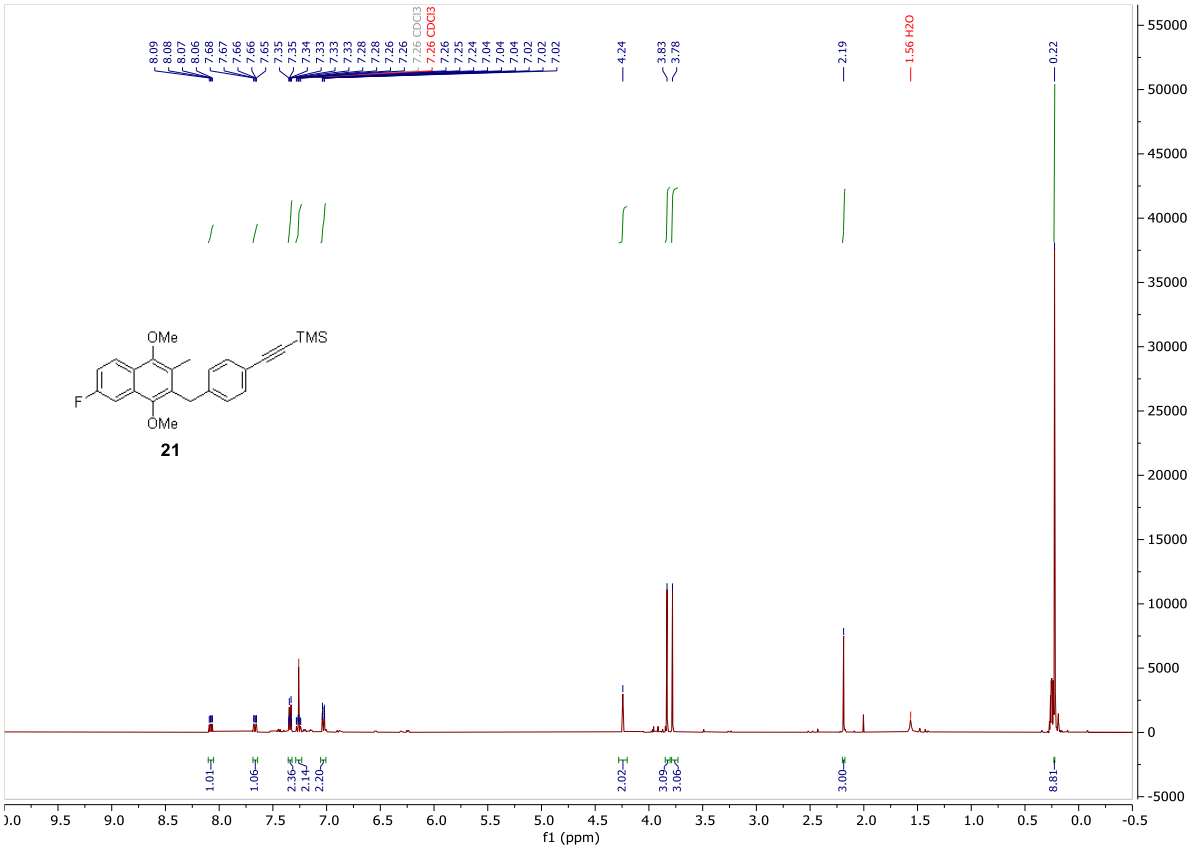

^{19}F {^{1}H} NMR (377 MHz, $CDCl_3$) – 21

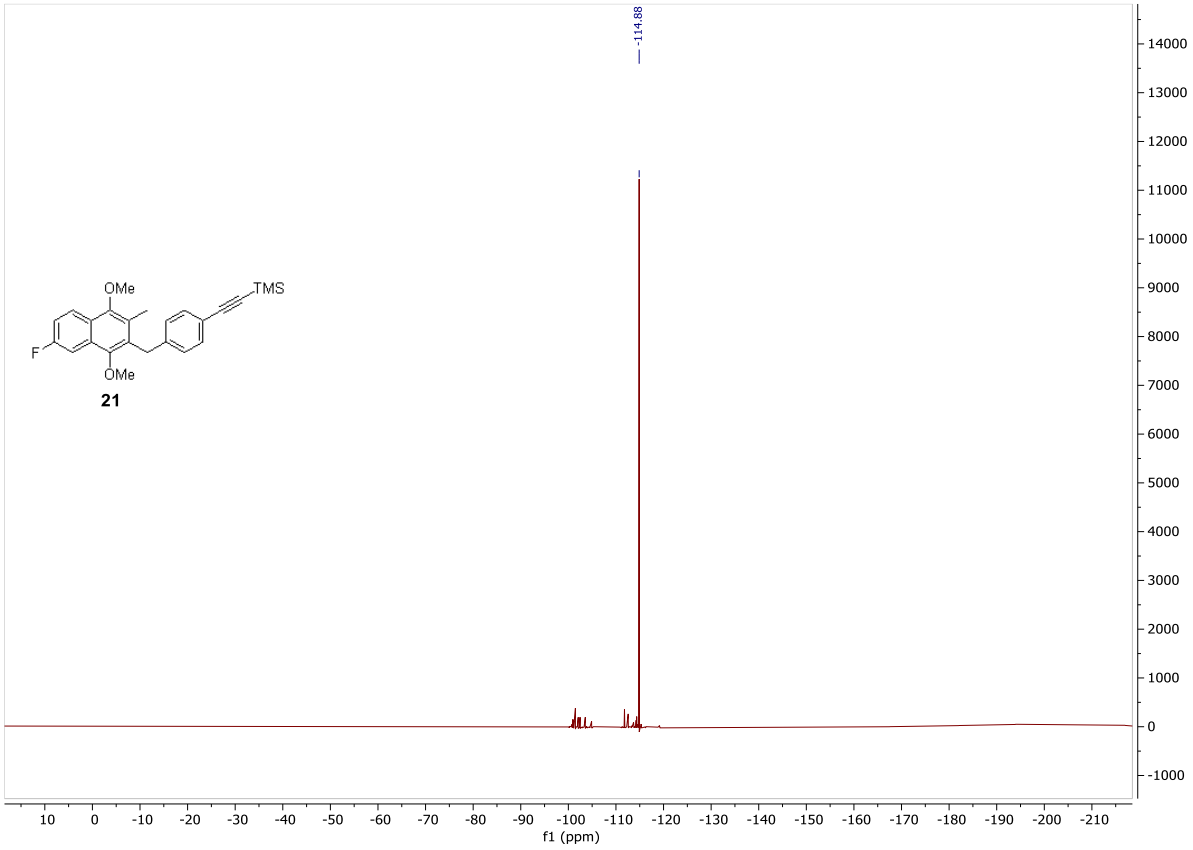

^{13}C {^{1}H} NMR (126 MHz, $CDCl_3$) – 21

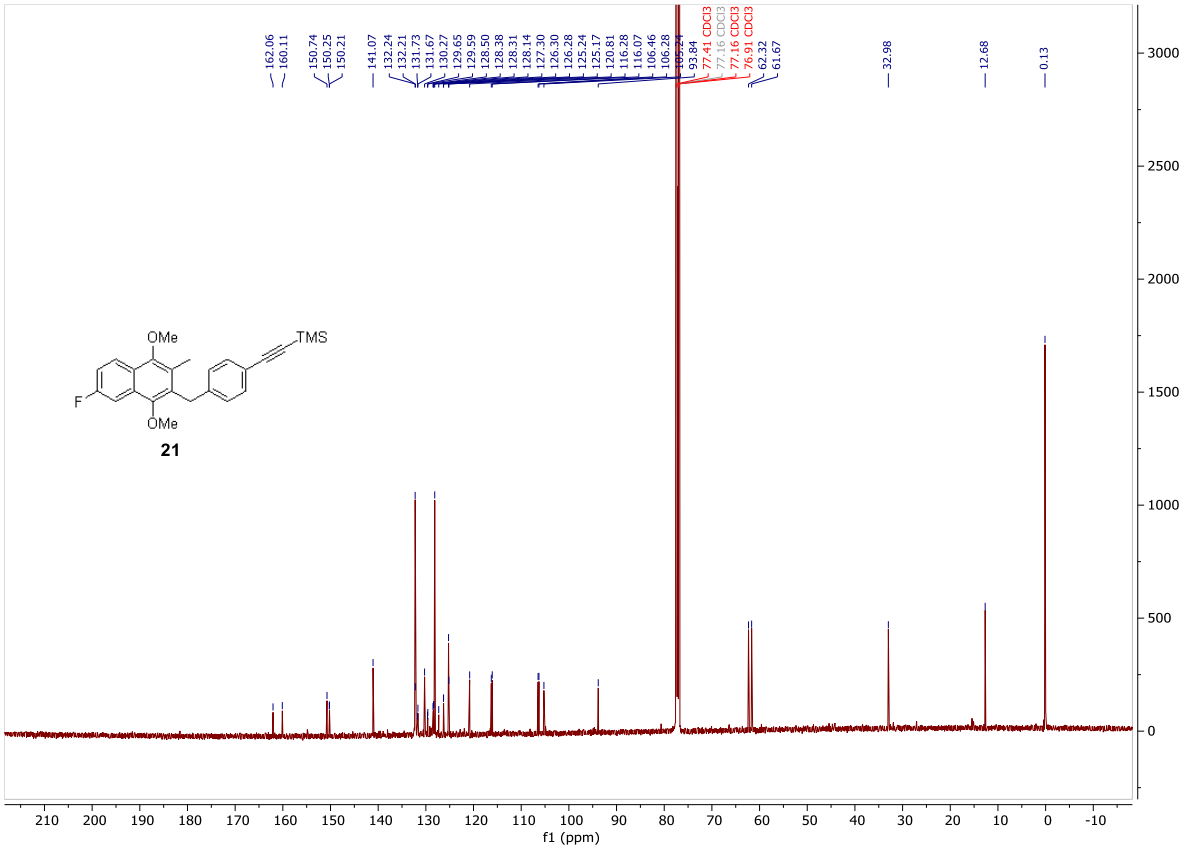

^{1}H NMR (400 MHz, $CDCl_3$) – 22

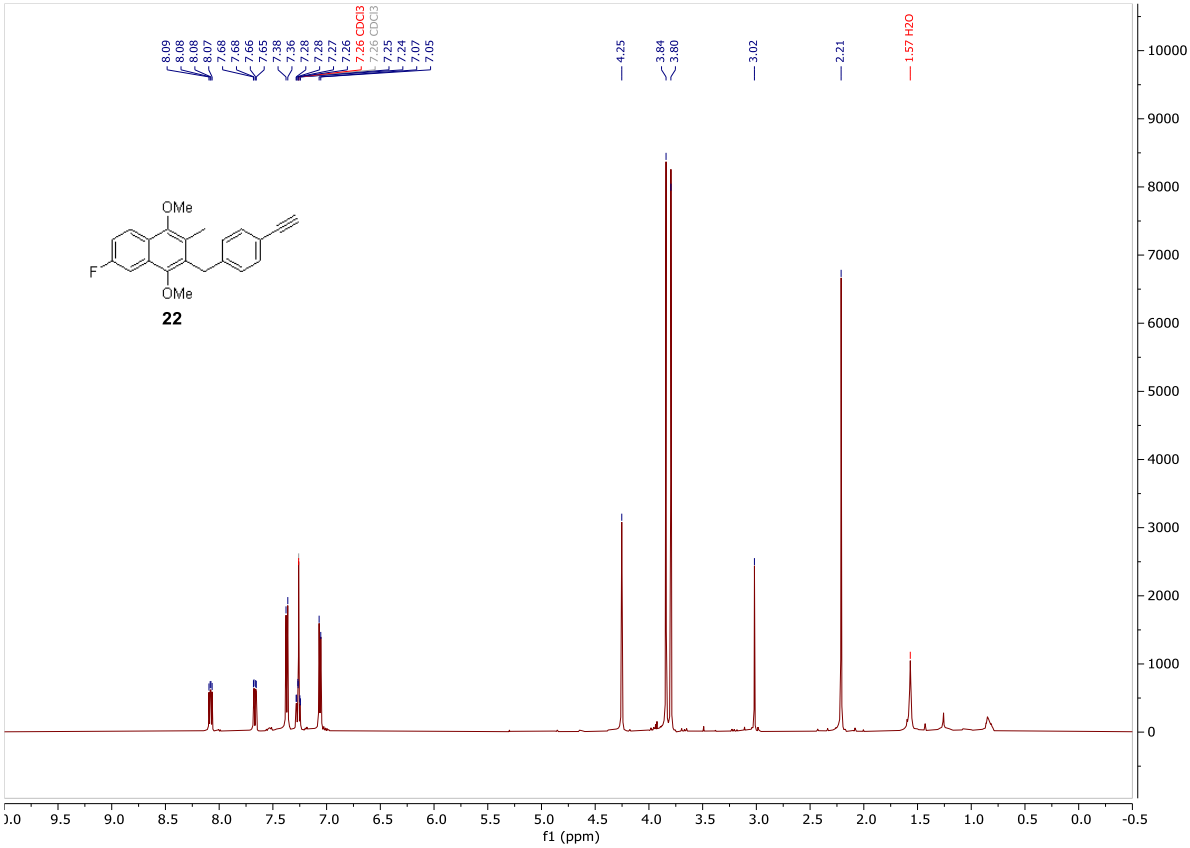

^{19}F {^{1}H} NMR (377 MHz, $CDCl_3$) – 22

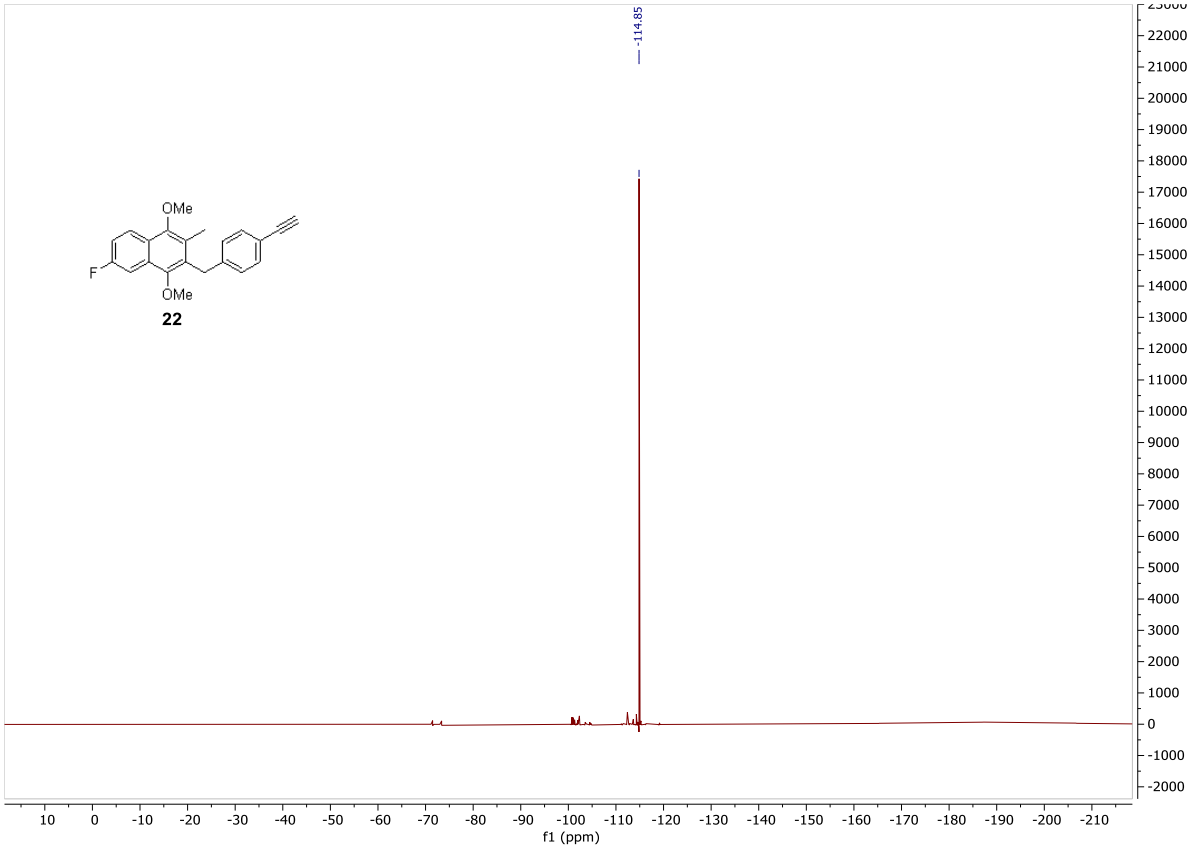

^{13}C {^{1}H} NMR (126 MHz, $CDCl_3$) – 22

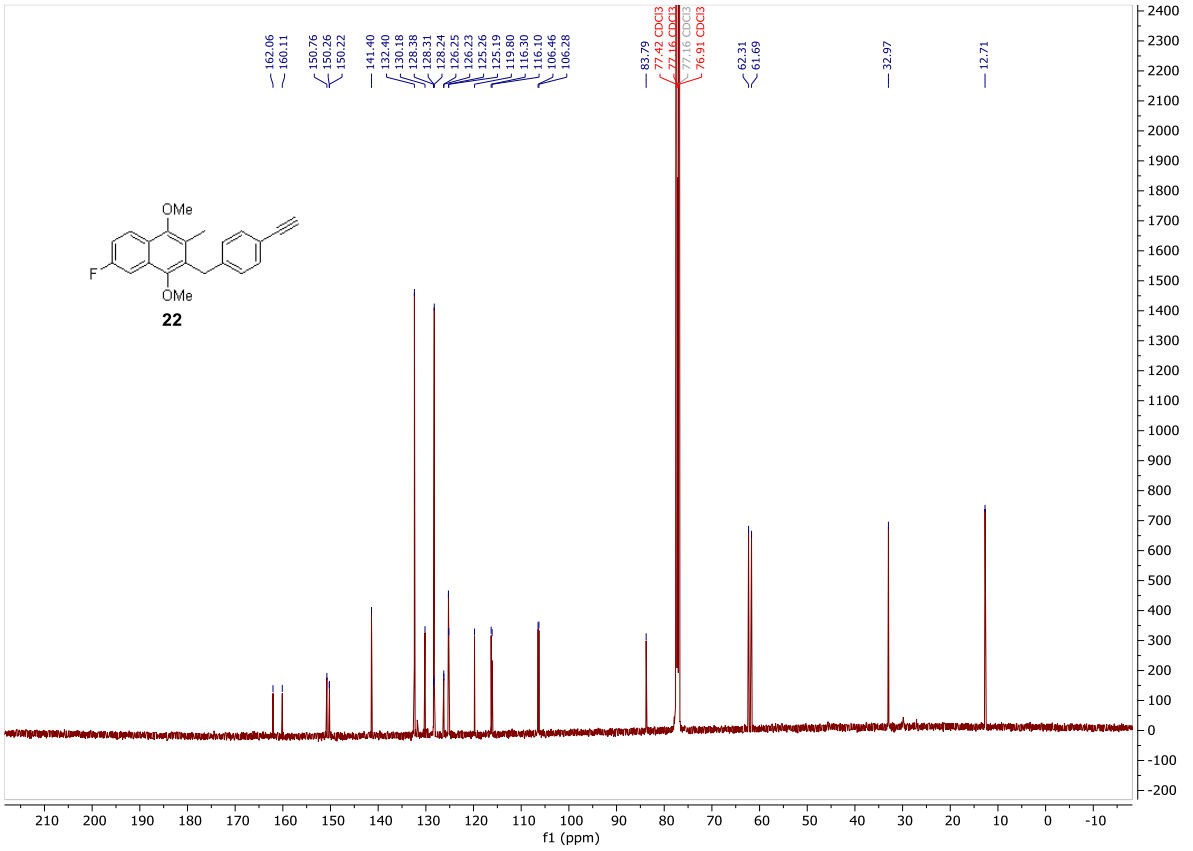

^{1}H NMR (400 MHz, $CDCl_3$) – 6-fluoro-PDO

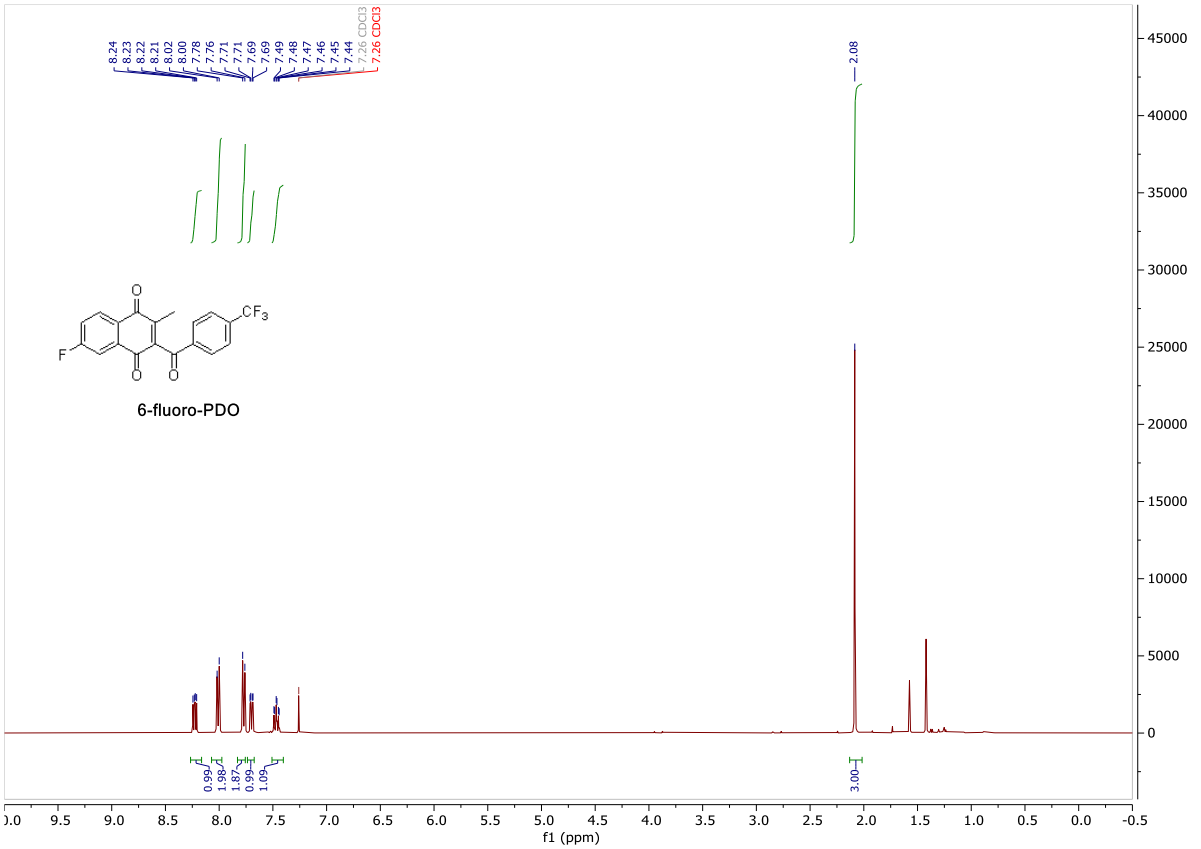

^{19}F {^{1}H} NMR (377 MHz, $CDCl_3$) – 6-fluoro-PDO

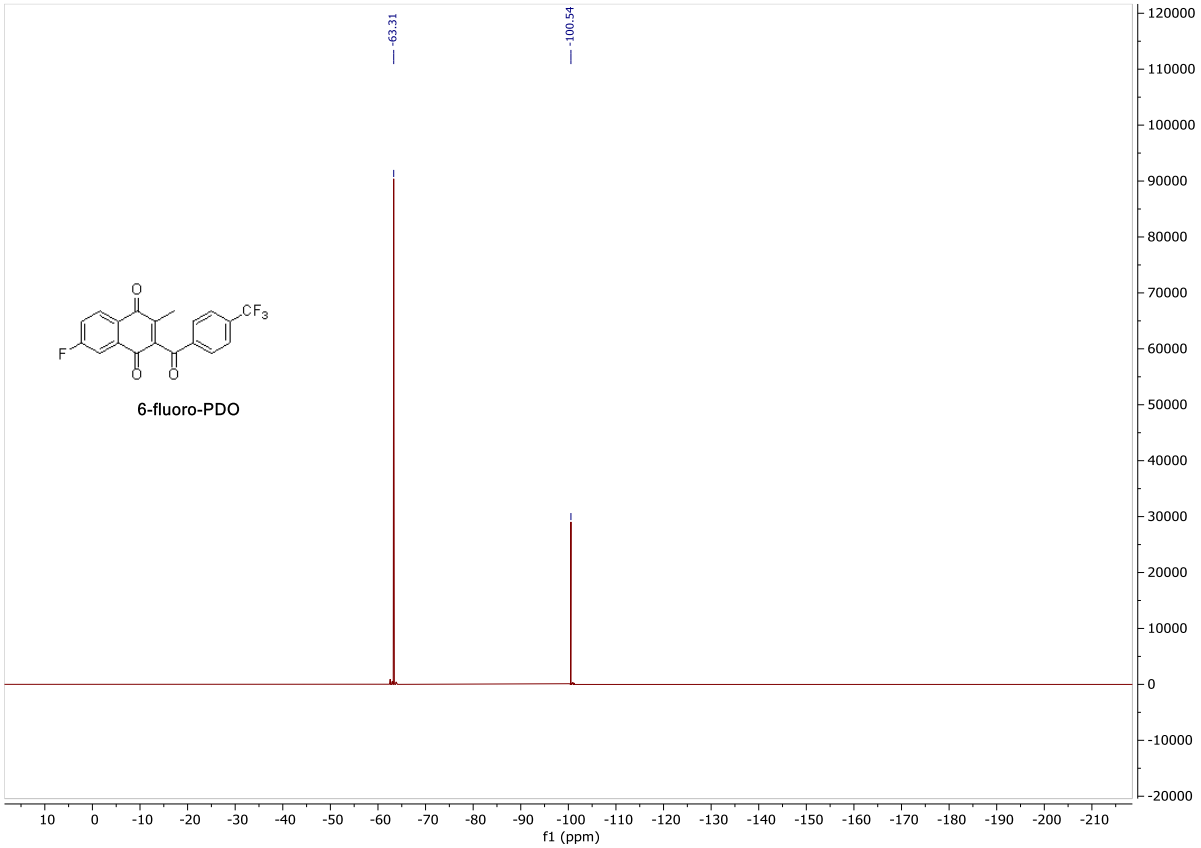

^{13}C {^{1}H} NMR (126 MHz, $CDCl_3$) – 6-fluoro-PDO